

Phase separation and universal scaling in markets: Fear and fragility

Anirban Chakraborti^{1,2,*}, Hrishidev³, Kiran Sharma⁴, and Hirdesh K. Pharsi⁵

¹School of Computational and Integrative Sciences, Jawaharlal Nehru University, New Delhi-110067, India

²Centro Internacional de Ciencias, Cuernavaca-62210, México

³Indian Institute of Science Education and Research, Pune-411008, India

⁴Chemical & Biological Engineering, Northwestern University, Evanston, Illinois-60208, USA

⁵Instituto de Ciencias Físicas, Universidad Nacional Autónoma de México, Cuernavaca-62210, México

*anirban@jnu.ac.in

ABSTRACT

One of the spectacular examples of a complex system is the financial market, which displays rich correlation structures among price returns of different assets. The eigenvalue decomposition of a correlation matrix into partial correlations – market, group and random modes, enables identification of dominant stocks or “influential leaders” and sectors or “communities”. The correlation-based network of leaders and communities changes with time, especially during market events like crashes, bubbles, etc. Using the *eigen-entropy* measure, computed from the *eigen-centralities* (ranks) of different stocks in the correlation-network, we extract information about the “disorder” (or randomness) in the market correlation and its different modes. The relative-entropy measures computed for these modes enable us to construct a “phase space”, where the different market events undergo “phase-separation” and display “order-disorder” transitions, as observed in critical phenomena in physics. We choose the US S&P-500 and Japanese Nikkei-225 financial markets, over a 32-year period, and study the evolution of the cross-correlation matrices and their corresponding eigen-entropies. One of the relative entropy measures displays “universal scaling” behavior with respect to the mean market correlation. Further, a functional of the relative entropy measure acts as a good gauge for the “market fragility” (minimum risk of the market portfolio) and the “market fear” (volatility index). This new methodology helps us to better understand market dynamics and characterize the events in different phases as anomalies, bubbles, crashes, etc. that display intriguing phase separation and universal scaling behavior.

Introduction

Financial markets have historically exhibited sharp and largely unpredictable drops at a systemic scale, which are termed “market crashes”^{1,2}. Such rapid changes or “phase transitions” (not in the strict thermodynamic sense of physics^{3,4}) may in some cases have been triggered by unforeseen stochastic events or exogenous shocks, or more often, they may have been driven by certain endogenous underlying processes^{5,6}. The recent global economic downturn in 2007-08 brought us both predicament and hope! Predicament, since the traditional theories in economics could not predict, nay even warn, the near complete breakdown of the global financial system. And we are yet to recover from its long-lasting effects on the global economy. Hope, since one can now witness signs of change in economic and financial thinking, including the very fact that there is deeper (and less understood) link between macroeconomics and finance^{7,8}, which certainly merits more attention.

A financial market is truly a spectacular example of a complex system that is generally composed of many constituents, which may be diverse in forms but largely interconnected, such that their strong inter-dependencies and emergent behavior change with time. Thus, it becomes almost impossible to describe the dynamics of the system through some simple mathematical equations, and so new tools and interdisciplinary approaches are needed^{9,10}. Hence, there has been a surge of efforts in using ideas from complexity theory^{11–15} to explain and understand economic and financial markets. New insights and concepts, such as networks, systemic risk, tipping points, contagion and resilience have surfaced in the financial literature and may have the potential for better monitoring of the highly interconnected macroeconomic and financial systems and, thus, may help anticipate future economic slowdowns or financial crises.

An interesting representation of the financial market has been in the form of a correlation-based network^{16–19}. This has given new and useful insights into the underlying patterns and mechanisms that drive the overall behavior of this seemingly unpredictable complex system. One can look at the cross-correlations between price return time series of various stocks in a particular time epoch and infer a temporal cross-section of the underlying network structure^{20,21} that evolves with time. There are multitudes of methods such as Minimum Spanning Trees, Planar Graphs, Asset Graphs to extract the network structure

from the correlation matrices^{22,23}. Recently, Pharasi et. al^{24,25} used the tools of random matrix theory to determine market states and confirmed that during a market crash all the stocks start behaving similarly and the whole market begins to act like a single huge cluster or community. In contrast, during a bubble period, a particular sector gets overpriced or over-performs, causing accentuation of disparities among the various sectors or communities. The eigenvalue decomposition of a correlation matrix into partial correlations – market, group and random modes²⁵, enables identification of dominant stocks (influential leaders) and sectors (communities). The correlation-based network of leaders and communities changes with time, especially during market events like crashes, bubbles, etc. Thus, if one were able to monitor the evolution of this network structure continuously^{24,26,27}, one would be able to acquire useful insights that would help in developing better investment strategies, manage risk and stress-test the global financial system.

Here, our aim is to extract information about the “disorder” (or randomness) in the market and its eigenmodes, using the entropy measure – *eigen-entropy*²⁸, computed from the *eigen-centralities* (ranks)^{21,29} of different stocks in the correlation-network. The relative-entropy measures computed for these eigenmodes enable us to construct a “phase space”, where the different market events undergo “phase-separation” (akin to many physical or biophysical phenomena^{30–34}) and display “order-disorder” transitions as in critical phenomena in physics^{3,4}. This type of behavior has never been recorded for financial markets, and is distinct from the two-phase behavior in financial markets reported earlier by Plerou et al.³⁵. One of the relative entropy measures displays “universal scaling” behavior with respect to the mean market correlation; there is a data collapse, which suggests that the fluctuations in price returns for different financial assets, varying across countries, economic sectors and market parameters, are governed by the same statistical law. This apparent universal behavior may motivate us to do further research as to determine which market forces are responsible for driving the market or are important for determining the price co-movements and correlations. Further, a functional of the relative entropy measure acts as a good market indicator, as it can gauge the market “fragility” (minimum risk of the market portfolio) and the “market fear” (volatility index). This new and simple methodology helps us to better understand market dynamics and characterize the events in different phases as anomalies, bubbles, crashes, etc. that display intriguing phase separation and universal scaling behavior. In addition, this may lead to a foundation for understanding scaling and universality in a broader context, and providing us with altogether new concepts not anticipated previously. This methodology may be generalized and used in other complex systems to understand and foresee tipping points (similar to market crashes and bubbles) and fluctuation patterns.

Results

In adaptive complex systems like financial markets^{24,25,36,37}, one usually studies the time evolution of the cross-correlation matrices computed from the price returns time-series (see Methods) for N stocks computed over different time-epochs of size M days. We denote the cross-correlation matrices as $C(\tau)$, where τ indicates the end date of the time-epoch. Our aim is to understand the statistical properties of these matrices and its eigen modes, and characterize them as different “phase points” in the phase space of eigen-entropies (see Methods). We then study the evolution of $C(\tau)$ and the eigen modes over different overlapping time-epochs, shifted by Δ days, for two different stock markets: United States of America S&P-500 (USA), and (b) Japan Nikkei-225 (JPN), over the period of thirty two years (1985–2016).

Fig. 1 shows the schematic diagram for computation of eigen-entropy from market returns. The plot of return time-series for arbitrarily chosen stocks (here three), with a chosen epoch (of size M days) ending on day τ for the computation of Pearson correlation coefficients is shown in Fig. 1 (A). Fig. 1 (B) shows four chosen cross-correlation matrices $C(\tau)$: Anomaly (06/01/1988), Bubble (01/09/2000), Crash (22/09/2011) and Normal (28/02/1985) periods, in the S&P-500 market; the stocks are arranged according to their sectors (abbreviations given in the Data description in Methods). As mentioned in the Methods section and illustrated in Fig. 1, we define $\mathbf{A} = |C|^2$ (matrix element-wise) and compute the eigen-centralities $\mathbf{p} = \{p_i\}$. Fig. 1 (C) shows the ranked (sorted) eigen-centralities $\{p_i\}$ of the normalized eigenvector corresponding to the maximum eigenvalue – anomalous (green circles), bubble (blue diamonds), crash (red triangles) and normal (grey stars) periods of the financial market. Fig. 1 (D) shows the evolution of the eigen-entropy ($H = -\sum_{i=1}^N p_i \ln p_i$), evaluated from the correlation matrices for the 32-year period 1985–2016.

The eigen-entropies may be computed (see Methods) from the full correlation C , market mode C_M and group-random mode C_{GR} . Fig. 2 (A) and (C) show the evolution of market returns $r(\tau)$, mean market correlations $\mu(\tau)$, and different eigen-entropies $H(\tau)$, $H_M(\tau)$, and $H_{GR}(\tau)$ (shown in different colors; see legend), for S&P-500 and Nikkei-225 markets, respectively. The vertical dashed lines correspond to some indicative dates for bubbles (blue) and crashes (red) (see Table 1). These eigen-entropies can then be used for the characterization of market events, such as bubbles and crashes. We used a *rolling mean* and *rolling standard deviation* (with a window size of 40 days), and computed the *standardized values* of eigen-entropies H^{Std} , H_M^{Std} and H_{GR}^{Std} . Fig. 2 (B) and (D) show the 3D-plots of the standardized values of eigen-entropy (H^{Std}) corresponding to the full (along z-axis), eigen-entropy (H_{GR}^{Std}) corresponding to the group-random (x-axis), and eigen-entropy (H_M^{Std}) corresponding to the market mode (along y-axis), for S&P-500 and Nikkei-225 markets, respectively. The sequence of seven frames (three frames before, the event (in black), and three frames after) display the “order-disorder” transitions in case

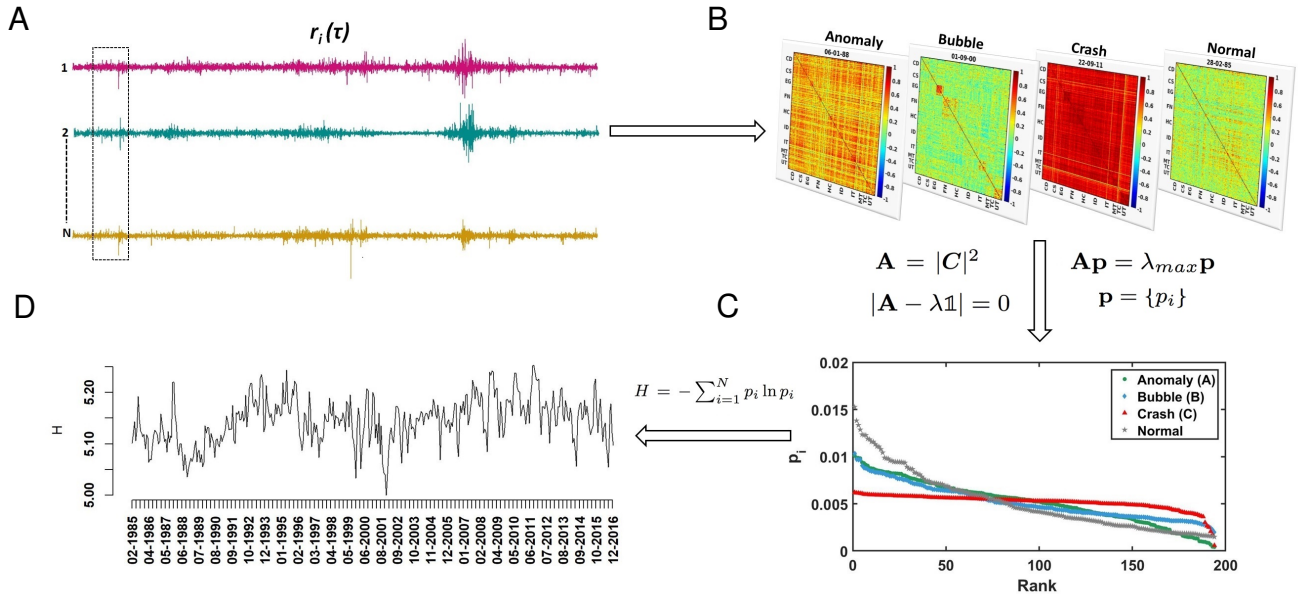


Figure 1. Schematic diagram for computation of eigen-entropy from market returns. (A) Return time-series plots for three arbitrarily chosen stocks (out of a total N stocks), with a chosen epoch (of size M days) ending on day τ for the computation of Pearson correlation coefficients. (B) Four chosen cross-correlation matrices $C(\tau)$: anomaly (06/01/1988), bubble (01/09/2000), crash (22/09/2011) and normal (28/02/1985) periods, in the S&P-500 market; the stocks are arranged according to their sectors. The sectoral abbreviations are: **CD**–Consumer Discretionary; **CS**–Consumer Staples; **EG**–Energy; **FN**–Financial; **HC**–Health Care; **ID**–Industrials; **IT**–Information Technology; **MT**–Materials; **TC**–Telecommunication Services; and **UT**–Utilities. We define $A = |C|^2$ (matrix element-wise) and use the characteristic equation $|A - \lambda \mathbb{1}| = 0$ to compute the eigenvalues $\{\lambda_1 \dots \lambda_N\}$; we denote the maximum eigenvalue as λ_{max} and the eigenvector corresponding to the maximum eigenvalue as p , such that $A p = \lambda_{max} p$. The normalized eigenvector has components: $p = \{p_i\}$, that are known as eigen-centralities. (C) The ranked (sorted) eigen-centralities $\{p_i\}$ of the normalized eigenvector corresponding to the maximum eigenvalue are plotted, for the anomalous (green circles), bubble (blue diamonds), crash (red triangles) and normal (grey stars) periods of the financial market. (D) Eigen-entropy ($H = -\sum_{i=1}^N p_i \ln p_i$), evaluated from the correlation matrices using a rolling epoch of $M = 40$ days and a shift of $\Delta = 20$ days, is plotted for the 32-year period 1985-2016.

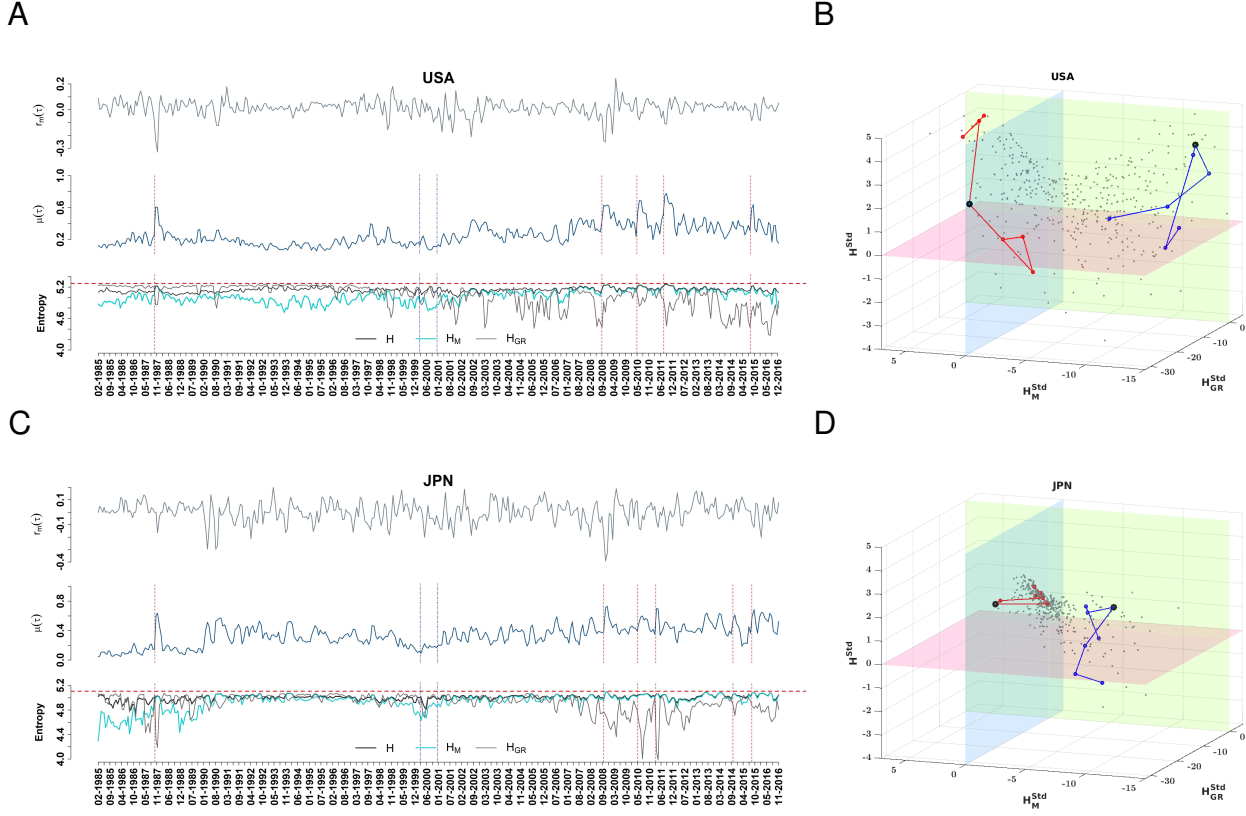


Figure 2. Evolution of market returns ($r(\tau)$), mean market correlations ($\mu(\tau)$), and eigen-entropies. The eigen-entropies are computed from the full correlation, market mode and group-random mode (shown in different colors; see legend), for (A) S&P-500 and (C) Nikkei-225 markets. **Order-disorder transitions around critical events.** The 3D-plots of the standardized values of eigen-entropy corresponding to the full correlation matrix H^{Std} (along z-axis), eigen-entropy corresponding to the group-random mode H_{GR}^{Std} (x-axis), and eigen-entropy corresponding to the market mode H_M^{Std} (along y-axis), for (B) S&P-500, and (D) Nikkei-225 markets. The sequence of seven frames display the “order-disorder” transitions around the main events (in black filled circle) – in case of bubble bursts (Dot-com in USA and JPN; shown in blue) and crashes (Lehman Brothers in USA and Fukushima in JPN; shown in red).

of bubble bursts (Dot-com in USA and JPN; shown in blue) and crashes (Lehman Brothers in USA and Fukushima in JPN; shown in red). Similar “order-disorder” transitions are observed in other crashes and bubbles for both USA and JPN (see Figs. S5-S6 and Table S1 in SI), emphasizing the universal character of the transitions and robustness of the method.

Fig. 3 shows evolution of relative-entropies and “phase separation” for S&P-500 and Nikkei-225 markets. We compute the relative-entropies $H - H_M$, $H - H_{GR}$, and $H_M - H_{GR}$, starting from the eigen-entropies corresponding to the full correlation, market mode and group-random mode, respectively. We then use these new variables to characterize and identify the different market events as anomalies, bubbles, bubble bursts, crashes and normal periods. Fig. 3 (B) and (D) show the 2D-plots of the phase space using relative-entropies $H - H_M$, and $H - H_{GR}$, for S&P-500 and Nikkei-225 markets, respectively. As evident, the epochs (event frames) clearly undergo “phase separation” – segregate into different market events: anomalies (green), bubbles (light blue), bubble bursts (blue), crashes (red) and normal (grey). The results can be compared to the benchmarks of WOE (see Figs. S3 and S7 in SI) for both USA and JPN. For the first time, we have been able to display such a phenomenon in the context of financial markets, which can be extremely significant for characterization and prediction of market events. The characterized events (corresponding to Fig. 3 (B) and (D)) are then indicated as vertical lines in the time-evolution plots in Fig. 3 (A) and (C). Interestingly, we find that many anomalies occur just around the major crashes, and intriguing patterns appear around the bubble formations and bubble bursts.

A “universal scaling” behavior is exhibited by the relative entropy $H - H_M$. The relative entropy $H - H_M$ versus mean market correlation μ is plotted in Fig. 4 (A) for S&P-500, (B) for Nikkei-225; the events are seen to lie on a straight line in a linear-logarithmic scale and the market event frames segregate into different portions: anomalies (green), bubbles (light blue), bubble bursts (blue), and crashes (red), interspersed by the normal events (grey). In Fig. 4 (C) the data for both markets collapse

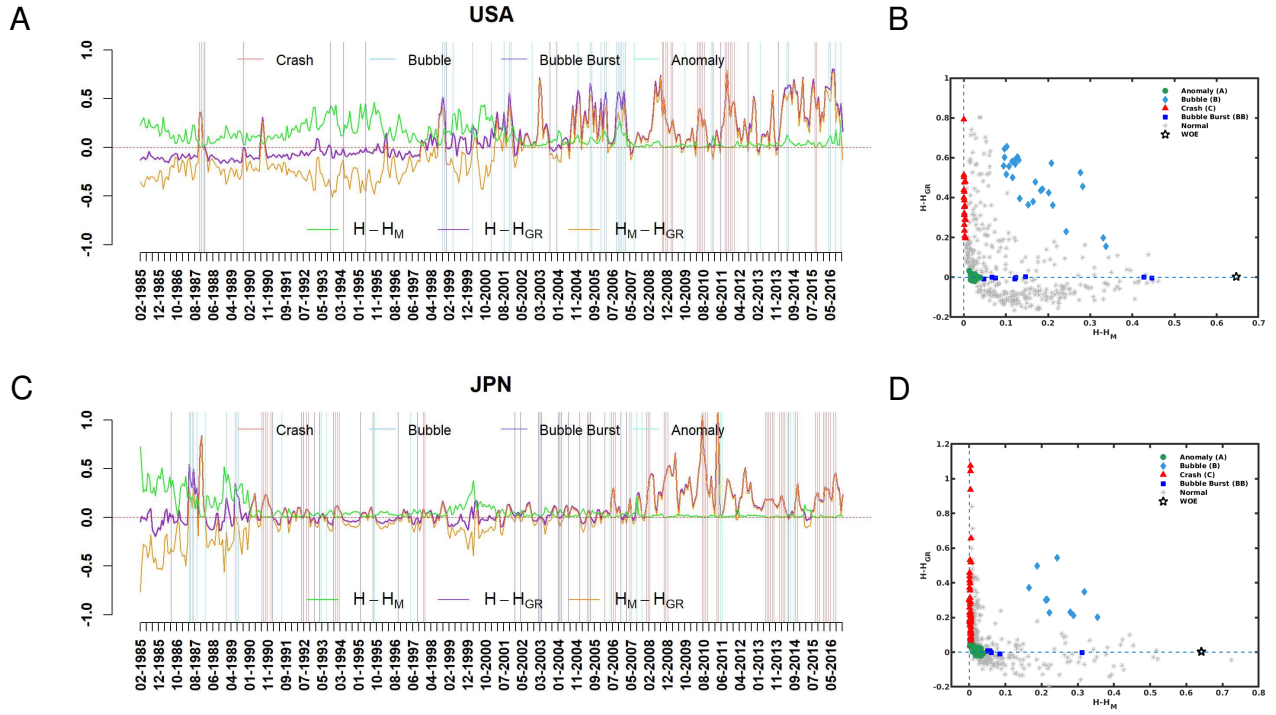


Figure 3. Evolution of relative-entropies. For (A) S&P-500 and (C) Nikkei-225 markets, the relative-entropies $H - H_M$, $H - H_{GR}$, & $H_M - H_{GR}$ are evaluated from the full, market and group-random mode to characterize and identify the different market events as anomalies, bubbles, bubble bursts, crashes and normal periods. **Phase separation.** The 2D-plots of the phase space using relative-entropies $H - H_M$ and $H - H_{GR}$, for (B) S&P-500, and (D) Nikkei-225 markets. The event frames show “phase separation” – segregation of different market events: anomalies (green), bubbles (light blue), bubble bursts (blue), crashes (red) and normal (grey). The black stars correspond to the benchmarks WOE in both USA and JPN.

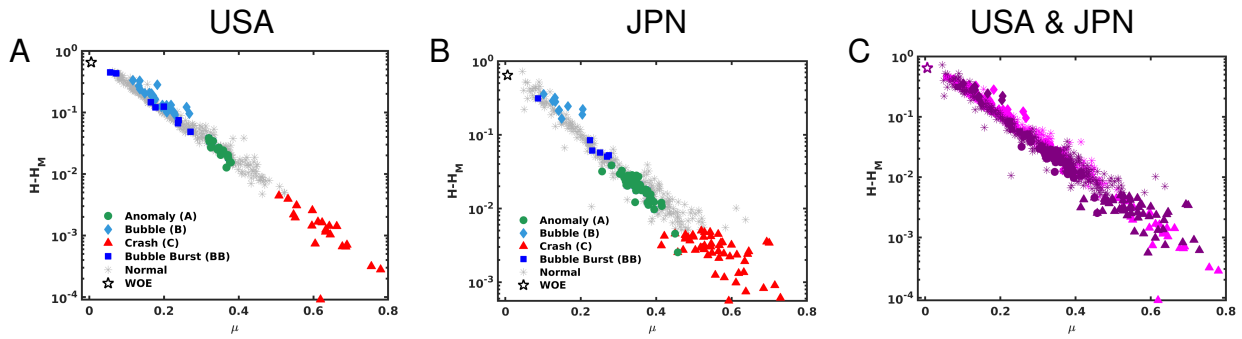


Figure 4. Scaling behavior of the relative entropy $H - H_M$. Plot of $H - H_M$ versus mean market correlation μ in linear-logarithmic scale for (A) S&P-500, and (B) Nikkei-225. The events are seen to lie on a straight line and the market event frames segregate into different portions: anomalies (green), bubbles (light blue), bubble bursts (blue), and crashes (red), interspersed by the normal events (grey). In (C), we see a data-collapse for both markets (USA in pink; JPN in purple) on a single curve, indicating a “universal scaling” behavior.



Figure 5. Evolution of the functional $-\ln(H - H_M)$ as compared to the mean correlation μ , volatility index VIX and minimum risk ρ . (A) The functional $-\ln(H - H_M)$ acts as a good indicator, as it can gauge the market fragility (minimum risk of the market portfolio) and the market fear (volatility index). (B) Cross-correlogram of the mean market correlation, functional of relative-entropy $-\ln(H - H_M)$, volatility index (market fear) and minimum risk (market fragility).

Table 1. Important Stock Market Events

Sl. No	Crisis	Period Date	Region Affected
1	Black Monday	1987-10-19	USA,JPN
2	Dot Com Bubble	1994-2000	USA,JPN
3	Lost Decade	2001-2010	JPN
4	US Housing Bubble	2005-2007	USA
5	Lehman Brothers Crash	2008-09-16	USA,JPN
6	DJ Flash Crash	2010-05-06	USA,JPN
7	Tsunami/Fukushima	2011-03-11	JPN
8	August 2011 Stock Markets Fall	2011-08-08	USA,JPN
9	Chinese Black Monday	2015-06-12	USA,JPN

on a single curve, which indicates universal scaling behavior normally seen in many physical systems^{38,39}. This implies that the co-movements in price returns for different financial assets and varying across countries, are governed by the same statistical law.

Very interestingly, this functional $-\ln(H - H_M)$ also acts as a good gauge for the market fragility (minimum risk of the market portfolio) and the market fear (volatility index). Fig. 5(A) shows the evolution of the functional $-\ln(H - H_M)$ as compared to the mean market correlation μ , volatility index VIX and minimum risk ρ . Fig. 5(B) displays the cross-correlogram of the mean market correlation, functional $-\ln(H - H_M)$, the minimum risk (market fragility) and volatility index (market fear). For a more elaborate cross-correlogram with many other indicators, see Table S2 in SI.

Summary and discussions

Here, we developed a general and robust methodology to extract information about the “disorder” (or randomness) in the market and its eigen modes, using the entropy measure – *eigen-entropy*, computed from the *eigen-centralities* (ranks) of different stocks in the correlation-network. We have used two different data sets of the stock markets USA S&P-500 and JPN Nikkei-225, spanning across a sufficiently long period of 32 years, to demonstrate its robustness.

We showed that the eigen-entropy is a simple yet robust prescription to quantify the disorder in a financial market. The methodology does not have any arbitrary thresholds. Further, the relative-entropy measures computed for these eigen modes enabled us to construct a “phase space”, where the different market events undergo “phase-separation” and display “order-disorder” transitions. The crashes occupy the region in the phase space, where $H - H_M \simeq 0$. During the crashes, the H and H_M almost touch the maximum disorder, $\ln N$ (corresponding to the random WOE). The events like “Dotcom bubble bursting” appear in the $H - H_{GR} \simeq 0$ axis. The events lying far away from the origin and axes are happening during bubble formation periods. The events lying close to the origin are like anomalies happening right before or right after major crashes. This type of phase-separation behavior in financial markets is being reported for the first time. Thus, we have here laid a clear

prescription for characterizing the market events as anomalies, bubbles, crashes, etc. using the relative entropy measures. It was not well-understood how and when bubbles form and when they burst. Our proposed methodology may help us to understand the market events and their dynamics, as well as find the time-ordering and appearances of the bubbles (formations or bursts) and crashes, separated by normal periods. We have studied the evolution of events around major crashes and bubbles (from historical records in USA and JPN; see *SI*). Of course, further studies are required.

We reiterate that our eigen-entropy measure has an advantage that it is uniquely determined and non-arbitrary (and also has less computational complexity). When one compared (for details, see *SI*, Fig. S8) our methodology with structural entropy²⁶, it is evident that the structural entropy is very sensitive to the community detection algorithm (different algorithms yield different community structures). Even the community detection algorithm⁴⁰, which involves identifying the group mode from the correlation matrix is not easy because the boundary (determined by the eigenvalues of the correlation matrix) between the random mode and the group mode, is not distinct (and often arbitrary).

Also, we have observed from the evolution of the entropy measures (H , H_M and H_{GR}) that the market behavior changes radically after 2000 (USA) and 1990 (JPN) corroborating to the findings of our earlier work²⁴, where we had found that the markets have “states” with different mean market correlation and market volatility.

Furthermore, the relative entropy $H - H_M$ displayed “universal scaling” behavior with respect to the mean market correlation μ ; a data-collapse was observed when plotted in a linear-logarithmic scale, which suggested that the fluctuations and co-movements in price returns for different financial assets and varying across countries are governed by the same statistical law. Also, the functional $-\ln(H - H_M)$ acted as a good indicator, as it could gauge market fragility (captured by the minimum risk of the market Markowitz portfolio) and the market fear (captured by the empirical volatility index). This can be important for managing risk and regulating the markets. In addition, these studies may lead to a deeper and broader understanding of scaling and universality phenomena in complex systems, in general.

Methods

Data Description

Price returns

We have used the adjusted closure price time series for United States of America (USA) S&P-500 index and Japan (JPN) Nikkei-225 index, for the period 02-01-1985 to 30-12-2016, from the Yahoo finance database⁴¹. USA has data for the $N = 194$ stocks and the period 02-01-1985 to 30-12-2016 ($T = 8068$ days). JPN has data for the $N = 165$ stocks and the period 04-01-1985 to 30-12-2016 ($T = 7998$ days). Note that we have included those stocks in our analyses, which are present in the data for the entire duration. It may also be noted that we have $T = 7897$ days data for the Nikkei-225 index whereas $T = 7998$ days data for stocks. So, we added zero return entries corresponding to the missing days in the time series of JPN index for the purpose of comparison, without affecting the results or conclusions.

The list of stocks (along with the sectors) for the two markets are given in the Table S3 and Table S4 in *SI*.

Volatility index

We have used the daily closure Volatility index (VIX) of the Chicago Board Options Exchange (CBOE) from Yahoo finance⁴¹ for the period 02-01-1990 to 30-12-2016, for $T = 6805$ days. It acts as a popular measure of the expectation of volatility in the stock market implied by the S&P-500 index “options”. It is computed and displayed on a real-time basis by the CBOE, and acts as the “fear index” or the “fear gauge”.

Cross-correlation Matrix

Returns series are constructed as $r_i(\tau) = \ln P_i(\tau) - \ln P_i(\tau - \Delta)$, where $P_i(\tau)$ is the adjusted closure price of stock i on day τ , and Δ is the shift in days. Instead of working with a long time series to determine the correlation matrix for N USA stocks, we work with a *short* time epoch of M days with a shift of Δ days. Then, the equal time Pearson correlation coefficients between stocks i and j is defined as $C_{ij}(\tau) = (\langle r_i r_j \rangle - \langle r_i \rangle \langle r_j \rangle) / \sigma_i \sigma_j$, where $\langle \dots \rangle$ represents the expectation value computed over the time-epochs of size M and the day ending on τ , and σ_k represents standard deviation of the k -th stock evaluated for the same time-epochs. We use $C(\tau)$ to denote the return correlation matrix for the time-epochs ending on day τ . Here, we show the results for $M = 40$ days with a shift of $\Delta = 20$ days (for other choices of M and Δ , see Fig. S1 in *SI*).

Eigen-centrality

Generally, for any given graph $G := (N, E)$ with $|N|$ nodes and $|E|$ edges, let $A = (a_{i,j})$ be the adjacency matrix, such that $a_{i,j} = 1$, if node i is linked to node j , and $a_{i,j} = 0$ otherwise. The relative centrality p_i score of node i can be defined as: $p_i = \frac{1}{\lambda} \sum_{v \in M(i)} p_j = \frac{1}{\lambda} \sum_{j \in G} a_{i,j} p_j$, where $M(i)$ is a set of the neighbors of node i and λ is a constant. With a small mathematical rearrangement, this can be written in vector notation as the eigenvector equation

$$A\mathbf{p} = \lambda \mathbf{p}.$$

In general, there may exist many different eigenvalues λ for which a non-zero eigenvector solution exists. We use the characteristic equation

$$|\mathbf{A} - \lambda \mathbf{1}| = 0$$

to compute the eigenvalues $\{\lambda_1 \dots \lambda_N\}$. However, the additional requirement that all the entries in the eigenvector be non-negative ($p_i \geq 0$) implies (by the Perron–Frobenius theorem) that only the maximum eigenvalue (λ_{max}) results in the desired centrality measure. The i^{th} component of the related eigenvector then gives the relative *eigen-centrality* score of the node i in the network. However, the eigenvector is only defined up to a common factor, so only the ratios of the centralities of the nodes are well defined. To define an absolute score one must *normalise* the eigenvector, such that the sum over all nodes N is unity, i.e., $\sum_{i=1}^N p_i = 1$. Furthermore, this can be generalized so that the entries in \mathbf{A} can be any matrix with real numbers representing the connection strengths. For correlation matrices $C(\tau)$, in order to enforce the Perron–Frobenius theorem, we work with $\mathbf{A} = |C_{i,j}|^n$, where $i, j = 1, \dots, N$ and n is any positive integer (we have used $n = 2$ in the paper; other values are discussed in SI; see also Fig. S2).

Eigenvalue decomposition of the empirical cross-correlation matrix

We have used the eigenvalue decomposition of the correlation matrices into market mode C_M , the group modes C_G and the random modes C_R and a composite group and random modes C_{GR} . From such a decomposition, it is also possible to reconstruct the correlation matrix as aggregates of the contributions of modes C_M , C_G , & C_R or C_M & C_{GR} as we show below.

In general, the correlation matrix of size $N \times N$ will have N eigenvalues, say $\{\lambda_1, \dots, \lambda_N\}$ arranged in descending order of magnitude. Then the maximum eigenvalue $\lambda_1 = \lambda_{max}$ of the correlation matrix, corresponds to a market mode that reflects the aggregate dynamics of the market common across all stocks, and strongly correlated to the mean market correlation μ . The group modes capture the sectoral behavior of the market, which are next few eigenvalues subsequent to the largest eigenvalue of the correlation matrix. Remaining eigenvalues capture the random modes behavior of the market (see Fig. S4). By using the eigenvalue decomposition, we can thus filter the true correlations (coming from the signal) and the spurious correlations (coming from the random noise).

For this, we first decompose the aggregate correlation matrix as

$$C = \sum_{i=1}^N \lambda_i e_i e_i' \quad (1)$$

where λ_i and e_i are the eigenvalues and eigenvectors, respectively, of the correlation matrix C . An easy way of handling the reconstruction of the correlation matrix is to sort the eigenvalues in descending order, and then rearranging the eigenvectors in corresponding ranks. This allows one to decompose the matrix into three separate components, viz., market, group and random

$$C = C_M + C_G + C_R, \quad (2)$$

$$= \lambda_1 e_1 e_1' + \sum_{i=2}^{N_G} \lambda_i e_i e_i' + \sum_{i=N_G+1}^N \lambda_i e_i e_i', \quad (3)$$

$$(4)$$

where N_G is the number of eigenvalues that satisfy the constraint $\lambda_+ \leq \lambda_G < \lambda_1$, with

$$\lambda_+ = \sigma^2 \left(1 + \frac{1}{\sqrt{Q}} \right)^2. \quad (5)$$

For empirical matrices, it is very difficult to determine the exact value of λ_+ and hence figure out N_G , for which the eigenvectors from 2 to N_G would describe the sectoral dynamics. Here, we choose $N_G = 20$ arbitrarily for the correlation decomposition (Fig. S4), corresponding to the 20 largest eigenvalues after the largest one.

In order to avoid the arbitrariness, we prefer the following decomposition:

$$C = C_M + C_{GR} \quad (6)$$

$$= \lambda_1 e_1 e_1' + \sum_{i=2}^N \lambda_i e_i e_i'. \quad (7)$$

Eigen-entropy

Following the tradition in information theory, we use the eigen-entropy $H = -\sum_{i=1}^N p_i \ln p_i$, since all the normalised eigen-centralities are non-negative ($p_i \geq 0$) and $\sum_{i=1}^N p_i = 1$, as explained above. The eigen-entropy may be described as kind of

measure of disorder or the degree of randomness in the matrix $\mathbf{A} = |C|^2$; higher the eigen-entropy, higher is the disorder in the matrix; the highest being in the case of WOE, where $H \sim \ln N$. If one assumes a network picture, when the network is complete, then the eigen-centralities of all nodes are uniform $p_i = 1/N$, and the maximum entropy $H_{max} = \ln N$ (corresponding to WOE); when none of the nodes are connected to each other, then minimum entropy $H_{min} = 0$. For realistic networks, the entropy will be bounded by these two limits.

Thus, corresponding to $\mathbf{A} = |C_M|^2$ (matrix element-wise) and $\mathbf{A} = |C_{GR}|^2$ (matrix element-wise), we have H_M and H_{GR} , respectively.

Minimum Risk Portfolio

We calculated the minimum risk portfolio in the Markowitz framework, as a measure of risk/fragility in the market. In this framework, it is assumed that rational investors with risk-aversion, will minimize

$$\omega' \Sigma \omega - \phi R' \omega$$

with respect to the weight vector ω . We denote Σ as the “covariance matrix” of the stock returns, R' as the expected return vector, and ϕ as a parameter that reflects the risk appetite of the investor. Further, we set the short-selling constraint such that $\omega_i \geq 0$ and ϕ equal to zero, for finding the minimal risk portfolio. This then entails a convex combination of stock returns; the other extreme would lead to a corner solution. For calculating this we have used a modified version a pre-written function from mathstack file exchange.

References

1. Buchanan, M. *Ubiquity: Why Catastrophes Happen* (Three Rivers Press, New York, 2000).
2. Sornette, D. *Why Stock Markets Crash: Critical Events in Complex Financial Systems* (Princeton University Press, 2004).
3. Stanley, H. E. *Phase transitions and critical phenomena* (Clarendon Press, Oxford, 1971).
4. Sethna, J. *Statistical mechanics: entropy, order parameters, and complexity*, vol. 14 (Oxford University Press, 2006).
5. Sorkin, A. R. *Too Big to Fail: The Inside Story of How Wall Street and Washington Fought to Save the Financial System and Themselves* (Viking, New York, 2009).
6. Acemoglu, D., Ozdaglar, A. & Tahbaz-Salehi, A. Systemic risk and stability in financial networks. *American Economic Review* **105**, 564–608 (2015).
7. Sharma, K., Gopalakrishnan, B., Chakrabarti, A. S. & Chakraborti, A. Financial fluctuations anchored to economic fundamentals: A mesoscopic network approach. *Scientific Reports* **7**, 8055 (2017).
8. Sharma, K., Chakrabarti, A. S. & Chakraborti, A. Multi-layered network structure: Relationship between financial and macroeconomic dynamics. In *New Perspectives and Challenges in Econophysics and Sociophysics*, 117–131 (Springer, 2019).
9. Vemuri, V. *Modeling of Complex Systems: An Introduction* (Academic Press, New York, 1978).
10. Gell-Mann, M. What is complexity? *Complexity* **1**, 16–19 (1995).
11. Mantegna, R. N. & Stanley, H. E. *An introduction to econophysics: correlations and complexity in finance* (Cambridge University Press, Cambridge, 2007).
12. Bouchaud, J.-P. & Potters, M. *Theory of Financial Risk and Derivative Pricing: from Statistical Physics to Risk Management* (Cambridge University Press, 2003).
13. Sinha, S., Chatterjee, A., Chakraborti, A. & Chakrabarti, B. K. *Econophysics: an introduction* (John Wiley & Sons, 2010).
14. Chakraborti, A., Muni Toke, I., Patriarca, M. & Abergel, F. Econophysics review: I. empirical facts. *Quantitative Finance* **11**, 991–1012 (2011).
15. Chakraborti, A. *et al.* Statistical mechanics of competitive resource allocation using agent-based models. *Physics Reports* **552**, 1–25 (2015).
16. Bonanno, G., Caldarelli, G., Lillo, F. & Mantegna, R. N. Topology of correlation-based minimal spanning trees in real and model markets. *Phys. Rev. E* **68**, 046130 (2003).
17. Onnela, J.-P., Kaski, K. & Kertész, J. Clustering and information in correlation based financial networks. *The European Physical Journal B* **38**, 353–362 (2004).
18. Tumminello, M., Di Matteo, T., Aste, T. & Mantegna, R. N. Correlation based networks of equity returns sampled at different time horizons. *The European Physical Journal B* **55**, 209–217 (2007).

19. Tumminello, M., Lillo, F. & Mantegna, R. N. Correlation, hierarchies, and networks in financial markets. *Journal of Economic Behavior & Organization* **75**, 40–58 (2010).
20. Newman, M. E., Barabási, A.-L. & Watts, D. J. *The structure and dynamics of networks* (Princeton University Press, Princeton, 2006).
21. Barabási, A.-L. *Network science* (Cambridge University Press, Cambridge, 2016).
22. Bonanno, G. *et al.* Networks of equities in financial markets. *The European Physical Journal B* **38**, 363–371 (2004).
23. Newman, M. E. *Networks: an introduction* (Oxford University Press, Oxford, 2010).
24. Pharasi, H. K. *et al.* Identifying long-term precursors of financial market crashes using correlation patterns. *New Journal of Physics* **20**, 103041 (2018).
25. Pharasi, H. K., Sharma, K., Chakraborti, A. & Seligman, T. H. *Complex Market Dynamics in the Light of Random Matrix Theory*, 13–34 (Springer International Publishing, Cham, 2019).
26. Almog, A. & Shmueli, E. Structural entropy: Monitoring correlation-based networks over time with application to financial markets. *Scientific reports* **9**, 10832 (2019).
27. Kuyyamudi, C., Chakrabarti, A. S. & Sinha, S. Emergence of frustration signals systemic risk. *Phys. Rev. E* **99**, 052306 (2019).
28. Fan, Y. *et al.* Lifespan development of the human brain revealed by large-scale network eigen-entropy. *Entropy* **19**, 471 (2017).
29. Albert, R. & Barabási, A.-L. Statistical mechanics of complex networks. *Reviews of Modern Physics* **74**, 47 (2002).
30. Mazurin, O. V. & Porai-Koshits, E. *Phase separation in glass* (Elsevier, 1984).
31. Lloyd, D. R., Kinzer, K. E. & Tseng, H. Microporous membrane formation via thermally induced phase separation. i. solid-liquid phase separation. *Journal of Membrane Science* **52**, 239 – 261 (1990).
32. Poole, P. H., Sciortino, F., Essmann, U. & Stanley, H. E. Phase behaviour of metastable water. *Nature* **360**, 324 (1992).
33. van de Witte, P., Dijkstra, P., van den Berg, J. & Feijen, J. Phase separation processes in polymer solutions in relation to membrane formation. *Journal of Membrane Science* **117**, 1 – 31 (1996).
34. Nagaev, E. L. *et al.* *Colossal magnetoresistance and phase separation in magnetic semiconductors* (World Scientific, 2002).
35. Plerou, V., Gopikrishnan, P. & Stanley, H. E. Two-phase behaviour of financial markets. *Nature* **421**, 130 (2003).
36. Onnela, J.-P., Chakraborti, A., Kaski, K., Kertesz, J. & Kanto, A. Dynamics of market correlations: Taxonomy and portfolio analysis. *Physical Review E* **68**, 056110 (2003).
37. Münnix, M. C. *et al.* Identifying states of a financial market. *Scientific Reports* **2**, 644 (2012).
38. Stanley, H. E. Scaling, universality, and renormalization: Three pillars of modern critical phenomena. *Reviews of modern physics* **71**, S358 (1999).
39. Norman, M. R. The challenge of unconventional superconductivity. *Science* **332**, 196–200 (2011).
40. MacMahon, M. & Garlaschelli, D. Community detection for correlation matrices. *Phys. Rev. X* **5**, 021006 (2015).
41. Yahoo finance database. <https://finance.yahoo.co.jp/> (2017). Accessed on 7th July, 2017, using the R open source programming language and software environment for statistical computing and graphics.
42. List of stock market crashes and bear markets. https://en.wikipedia.org/wiki/List_of_stock_market_crashes_and_bear_markets (2019). Accessed on 7th July, 2019.
43. Bull markets. <https://bullmarkets.co/u-s-stock-market-in-1996/> (2019). Accessed on 7th July, 2019.
44. United states housing bubble. https://en.wikipedia.org/wiki/United_States_housing_bubble (2019). Accessed on 7th July, 2019.
45. A short history of stock market crashes. <https://www.cnbc.com/2016/08/24/a-short-history-of-stock-market-crashes.html> (2019). Accessed on 7th July, 2019.
46. Stock market selloff. https://en.wikipedia.org/wiki/2015-16_stock_market_selloff (2019). Accessed on 7th July, 2019.

47. Fortunato, S. Community detection in graphs. *Physics reports* **486**, 75–174 (2010).
48. Girvan, M. & Newman, M. E. Community structure in social and biological networks. *Proceedings of the National Academy of Sciences* **99**, 7821–7826 (2002).

Acknowledgements

The authors are grateful to Anindya S. Chakrabarti and Francois Leyvraz for their critical inputs and suggestions. H.K.P. is grateful for financial support provided by UNAM-DGAPA and CONACYT Proyecto Fronteras 952. A.C. and K.S. acknowledge support from the project UNAM-DGAPA-PAPIIT AG 100819 and CONACyT Project FRONTERAS 201.

Author contributions statement

A.C. designed research; A.C., H., K.S. and H.K.P. performed research; H., K.S., and H.K.P. analyzed data and prepared the figures; A.C. wrote the manuscript with input from all authors.

Supplementary information

We present the supplementary information to the methodology used in the paper, especially with respect to the variations of different parameters that affect the calculation and understanding of eigen-entropy H .

We also present some detailed analyses of benchmark comparisons with the Wishart Orthogonal Ensemble (WOE) and the critical events (bubbles and crashes) in USA and JPN. The table of major events (bubbles and crashes) is given in Table S1. The tables for the lists of stocks of USA and JPN are given in Table S3 and Table S4, respectively.

Finally, we also make a very brief comparison of the measures: eigen-entropy H that we propose in this paper, with the structural entropy S that was recently introduced by Almog et al.²⁶.

Methodology

Effects of the variation of the epoch size M and shift Δ

The continuous monitoring of the market can be done by dividing the total time series data into smaller epochs of size M . The corresponding correlation matrices generated from these smaller epochs are used for calculating the eigen-entropy H . In Fig. S1, we investigate the effects of the variation of parameters, epoch size M and shift Δ .

We observe that either the increase in the epoch M or shift Δ makes the time series plot of H more smooth (less fluctuations), and vice versa. The choice of these parameters are thus arbitrary to some extent, depending on the research questions and time scale we are interested.

Effect of the variation in the powers of correlation matrices $|C|^n$

Instead of taking the square of individual elements of the correlation matrix C , to make all the elements non-negative, we can also use the even powers or the odd powers of absolute values to accomplish the same. The effect of the same is shown in the Fig. S2. As observed the values of eigen-entropy H differ with the variation of the power n of correlation matrices. This is due to the fact that with the increase in power, the dissimilarities in the elements of the correlation matrix are amplified which will then in turn changes the centrality of the matrix. For very high powers the transformed correlation matrices will act like an adjacency matrix with very high values (close to 1s) and very low values (close to 0s).

It is also interesting to note that, depending on the problem, we can decide the range of correlations to focus on by adjusting the power of the elements of the correlation matrix.

Results

Correlation matrix decomposition and Wishart Orthogonal Ensemble Results

Fig. S3 (A) shows the plot of sorted eigen-centralities p_i against rank, computed from the normalized eigenvectors corresponding to the maximum eigenvalues for 1000 independent realizations of a Wishart orthogonal ensemble (WOE). Filled black squares represent the mean eigen-centralities computed from 1000 independent realizations of the WOE, that serves as a reference (the maximum disorder or randomness) in the market correlation with $N = 194$. Fig. S3 (B) shows the plot of the variation of eigen-entropy H as a function of system size (correlation matrix size) N , where each point represents a mean computed from 1000 independent realizations of an uncorrelated WOE. The theoretical curve (red dash) shows the variation $\sim \ln N$. Fig. S3 (C) shows the histograms of the eigen-centralities p_i for typical Anomaly (06/01/1988) (green circles), Bubble (01/09/2000) (blue diamonds), Crash (22/09/2011) (red triangles) and Normal (28/02/1985) (grey stars) and WOE (black squares).

For any matrix, we can perform the eigenvalue decomposition (see Methods). Fig. S4 shows the eigenvalue decompositions of the correlation matrices, for (A) normal, (B) anomalous, (C) bubble, (D) crash periods of the financial market, corresponding to the frames in Fig. 1, and in addition (E) shows the results for a random matrix taken from a Wishart orthogonal Ensemble (WOE), where we have denoted the different matrices as: full correlation C , market mode C_M , group mode C_G , random mode C_R , group-random mode C_{GR} and displayed the results in Fig. S4 (Left to Right). The last column shows the results for the ranked eigen-centralities p_i of the different correlation modes: full (C in black curve), market mode (C_M in turquoise curve) and group-random mode (C_{GR} in grey curve). Interestingly, for a normal period, the three curves are distinct and there are hierarchies in ranks in all curves; for the market anomaly, all the three curves almost coincide; for the bubble period, the curves corresponding to the full and the group-random modes coincide while there is a strict hierarchy in the eigen-centralities of the market mode; for crash period, the curves corresponding to the full and the market modes coincide while there is a strict hierarchy in the eigen-centralities of the group-random mode; and for the WOE, once again the curves corresponding to the full and the group-random modes coincide while there is a strict hierarchy in the eigen-centralities of the market mode. This feature is then exploited in characterizing the anomalies, bubbles, crashes and normal periods in the market, with the help of the corresponding entropy functions as explained below and displayed in Fig. 2 and Fig. 3.

Study of critical events (Crashes and Bubbles)

For the events listed in Table S1, we look at the frames around that particular event and see how it moves around in the phase space in Fig.S5 and Fig.S6.

Once we are able to characterize the epochs (event frames) into different “phases”, we can create the different ensembles of anomalies, bubbles, bubbles bursts, crashes and normal events. For each type of event, we find that eigen-centralities have distinct ranges of values and the sorted eigen-centrality curves have interesting features (hierarchies) in the eigenmodes. The eigen-entropies actually quantify these features appropriately. For the S&P-500 and Nikkei-225 markets, we compute the histograms of the eigen-centralities p_i . Fig. S7 shows the histograms (for S&P-500 (Top) and Nikkei-225 (Bottom)) for all the characterized anomalies (green circles), bubbles (light blue diamonds), bubble bursts (blue squares), crashes (red triangles),

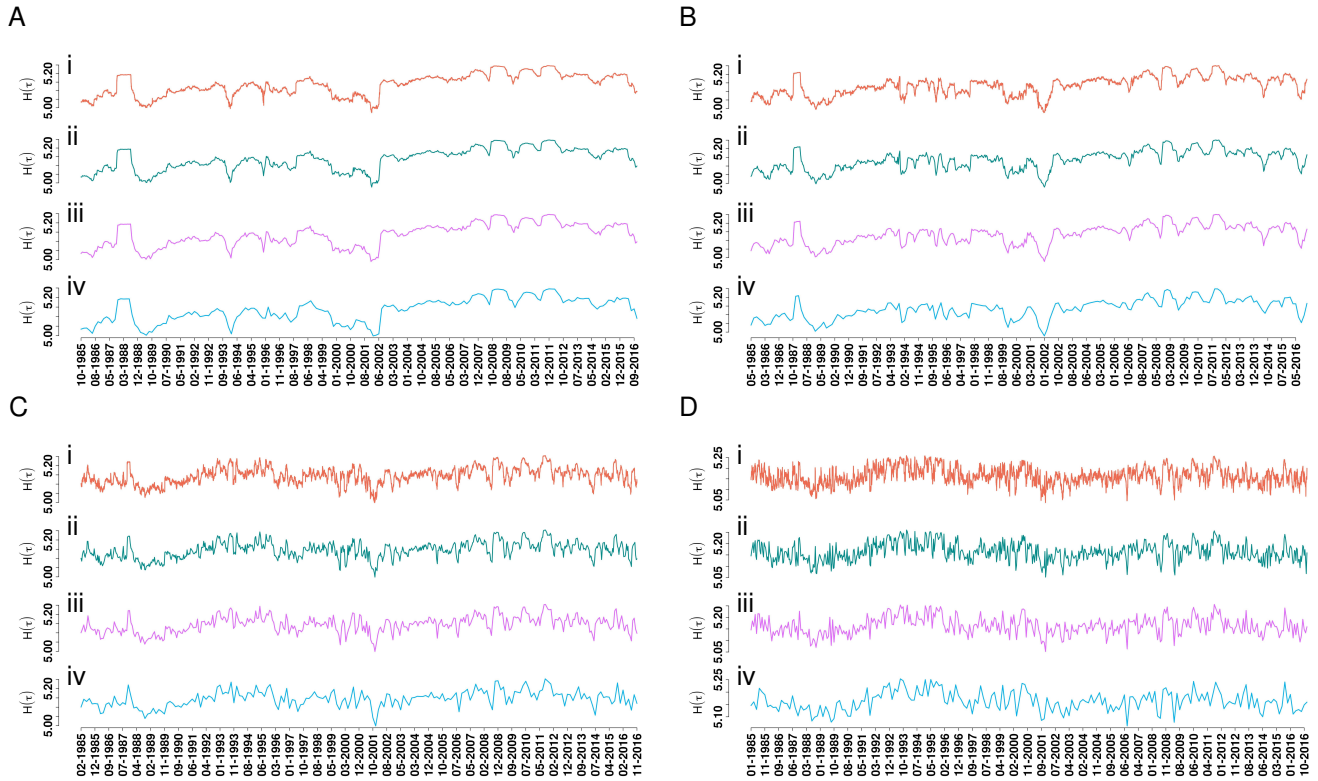


Figure S1. Effects of epoch size M and shift Δ on the time series of eigen-entropy H . The evolution of eigen-entropy H is calculated from correlation matrices corresponding to four different time epochs (A) $M = 200$, (B) $M = 100$, (C) $M = 40$, and (D) $M = 20$ days and each with four different shifts (i) $\Delta = 1$ day, (ii) $\Delta = 10$ days, (iii) $\Delta = 20$ days, and (iv) $\Delta = 40$ days over a period of 1985-2016. The fluctuations (local) of the eigen-entropy H are smoothened (smaller) for bigger shifts Δ .

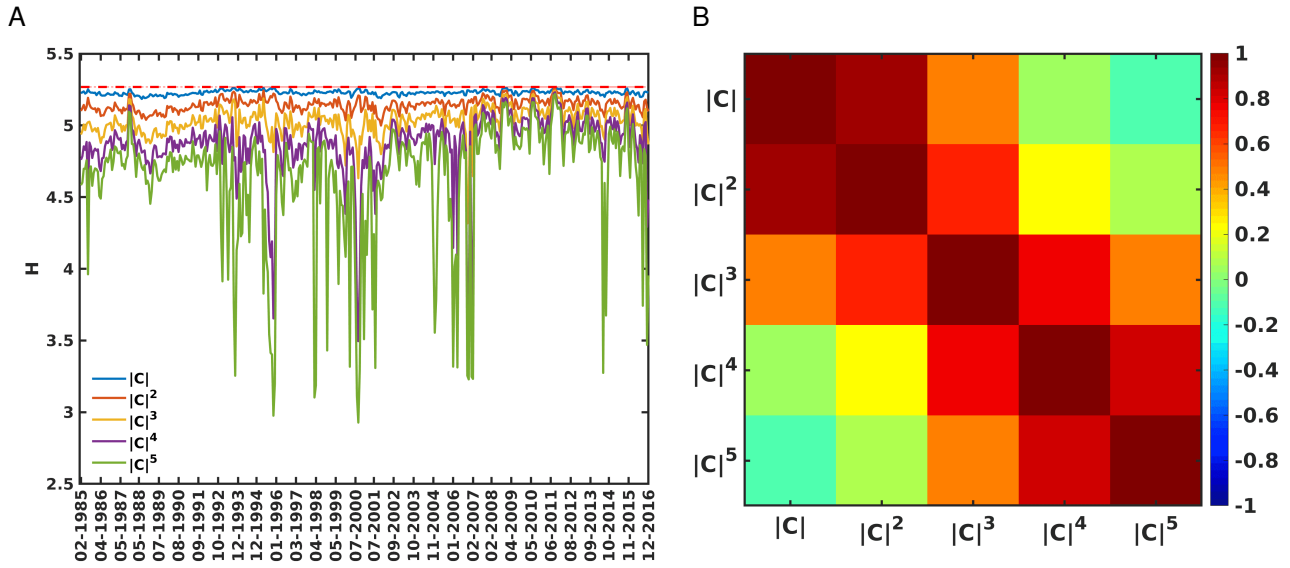


Figure S2. Comparison of the variation of n for $|C|^n$. The eigen-entropy H is calculated for different powers n of correlation matrix C by raising the elements of C to even powers or the absolute value of C to odd powers. (A) shows the time series of the eigen-entropies H of the correlation matrices of epoch $M = 40$ days and $\Delta = 20$ days for five different powers upto $n = 5$. The correlations among these five time series of eigen-entropy H is shown in (B).

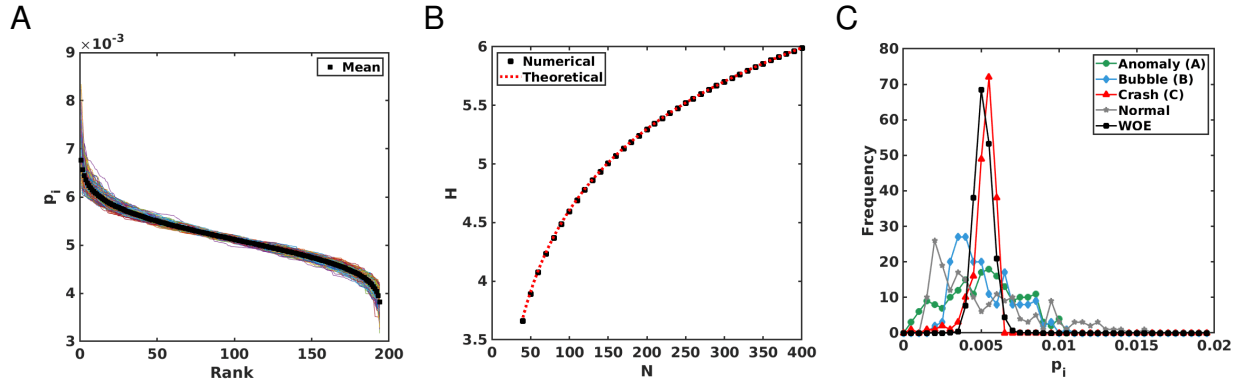


Figure S3. Eigen-centralities (ranks) and eigen-entropy. (A) Plots of sorted eigen-centralities p_i against rank, computed from the normalized eigenvectors corresponding to the maximum eigenvalues for 1000 independent realizations of a Wishart orthogonal ensemble (WOE). Filled black squares represent the mean eigen-centralities computed from 1000 independent realizations of the WOE, that serves as a reference (the maximum disorder or randomness) in the market correlation with $N = 194$. (B) Plot showing the variation of eigen-entropy H as a function of system size (correlation matrix size) N , where each point represents a mean computed from 1000 independent realizations of a WOE. The theoretical curve (red dash) shows the variation $\sim \ln N$. (C) Histograms of the eigen-centralities p_i for typical anomalous (green circles), bubble (blue diamonds), crash (red triangles) and normal (grey stars) and WOE (black squares).

normal events (grey stars), averaged over the respective ensembles, for the full/decomposed matrices. For comparison, we also plot the results for the WOE (black squares). This helps us understand what actually happens in the market, during these different types of events (phases) and what type of hierarchies exist within the stocks's eigen-centralities. This would shed new light into the understanding of formation of bubbles, development of bursts and crashes, etc.

Cross-correlogram of the entropy measures with market parameters

Comparison with structural entropy S

Recently, the measure of structural entropy S was introduced for the extraction of information from a correlation-based network in the form of a single representative value^{26,40}. One finds that evolution of structural entropy may provide information about

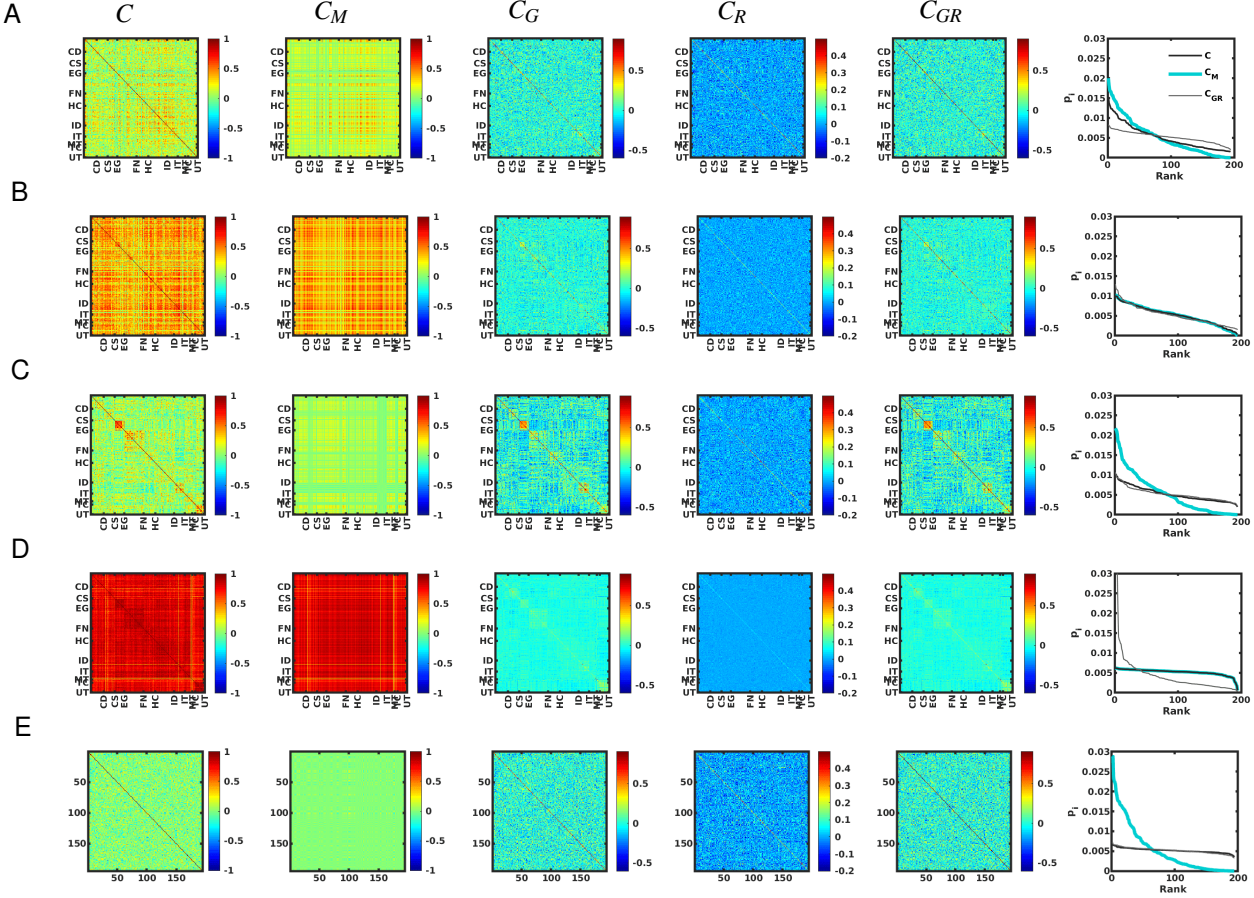


Figure S4. Eigenvalue decomposition of the correlation matrices. For (A) normal, (B) anomalous, (C) bubble, (D) crash periods of the financial market, as in Fig. 1, and (E) random matrix taken from uncorrelated WOE. (Left to right) Plots showing the correlation matrices: full C , market mode C_M , group mode C_G , random mode C_R , group-random mode C_{GR} and the ranked eigen-centralities p_i of the different correlation modes: full (C in black curve), market mode (C_M in turquoise curve) and group-random mode (C_{GR} in grey curve). Interestingly, for a normal period, the three curves are distinct and there are hierarchies in ranks in all curves; for the market anomaly, all the three curves almost coincide; for the bubble period, the curves corresponding to the full and the group-random modes coincide while there is a strict hierarchy in the eigen-centralities of the market mode; for crash period, the curves corresponding to the full and the market modes coincide while there is a strict hierarchy in the eigen-centralities of the group-random mode; and for the WOE, once again the curves corresponding to the full and the group-random modes coincide while there is a strict hierarchy in the eigen-centralities of the market mode. This feature is then exploited in characterizing the market events into anomalies, bubbles, crashes, normal periods, etc. with the help of the corresponding entropy functions as in Fig. 2 and Fig. 3.

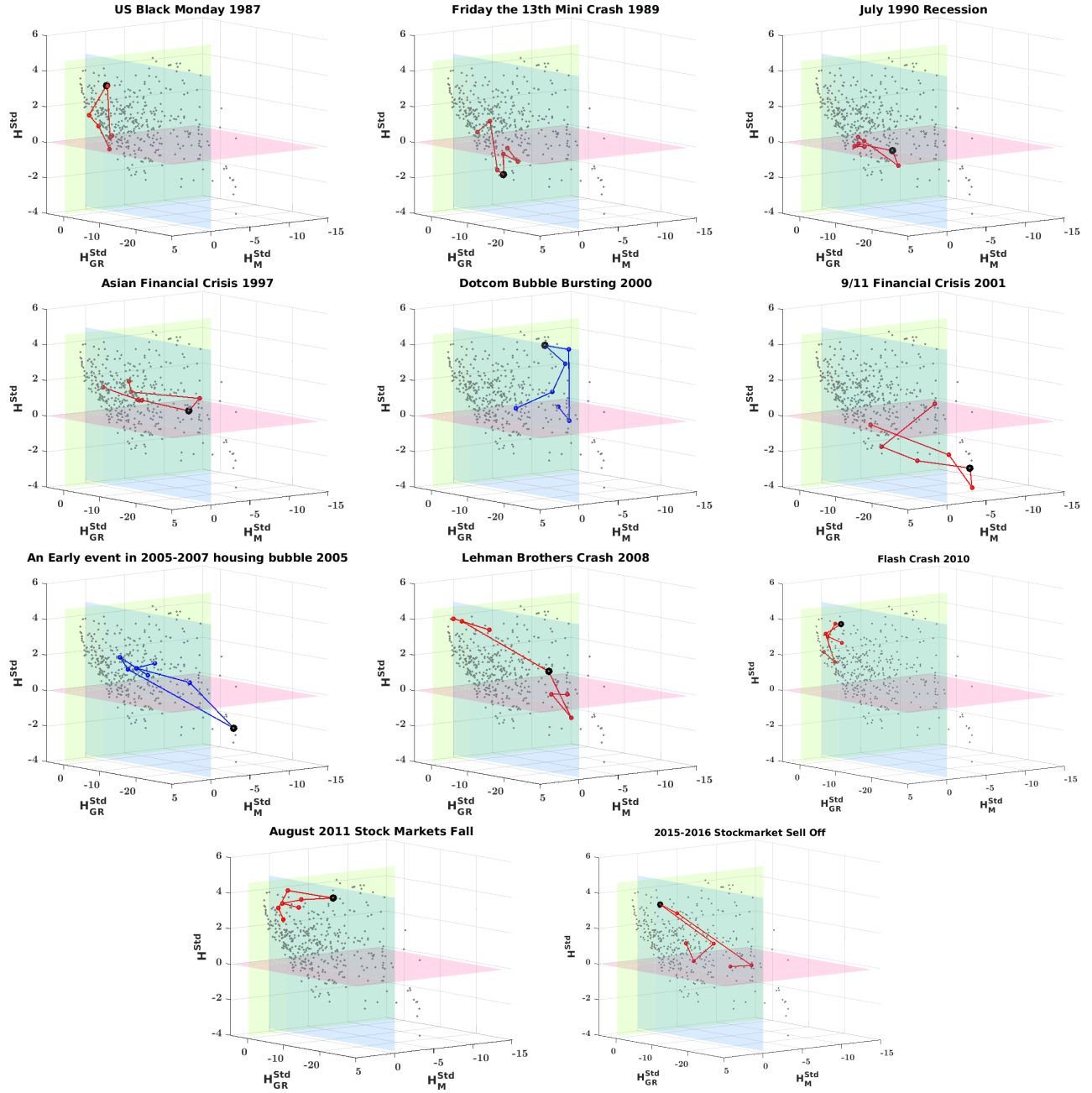


Figure S5. Evolution around the important events in USA market. Eigen-entropy H calculated from the correlation matrices: (full) C , market mode C_M and group-random mode C_{GR} for all the frames (epoch $M = 40$ days and shift $\Delta = 20$ days) over a period of 1985-2016 of USA (S&P-500). After standardizing the variables with moving average and moving standard deviation, each frame (grey dot) is embedded in a 3-D space with axes H^{std}_M , H^{std}_{GR} and H^{std}_C . Eleven important events with seven frames around those events (three before and three after the event) were taken from the history and shown in the plots. Bubbles are connected with blue line and other critical events with red lines. The frame containing the important event is marked with black circle for better visibility.

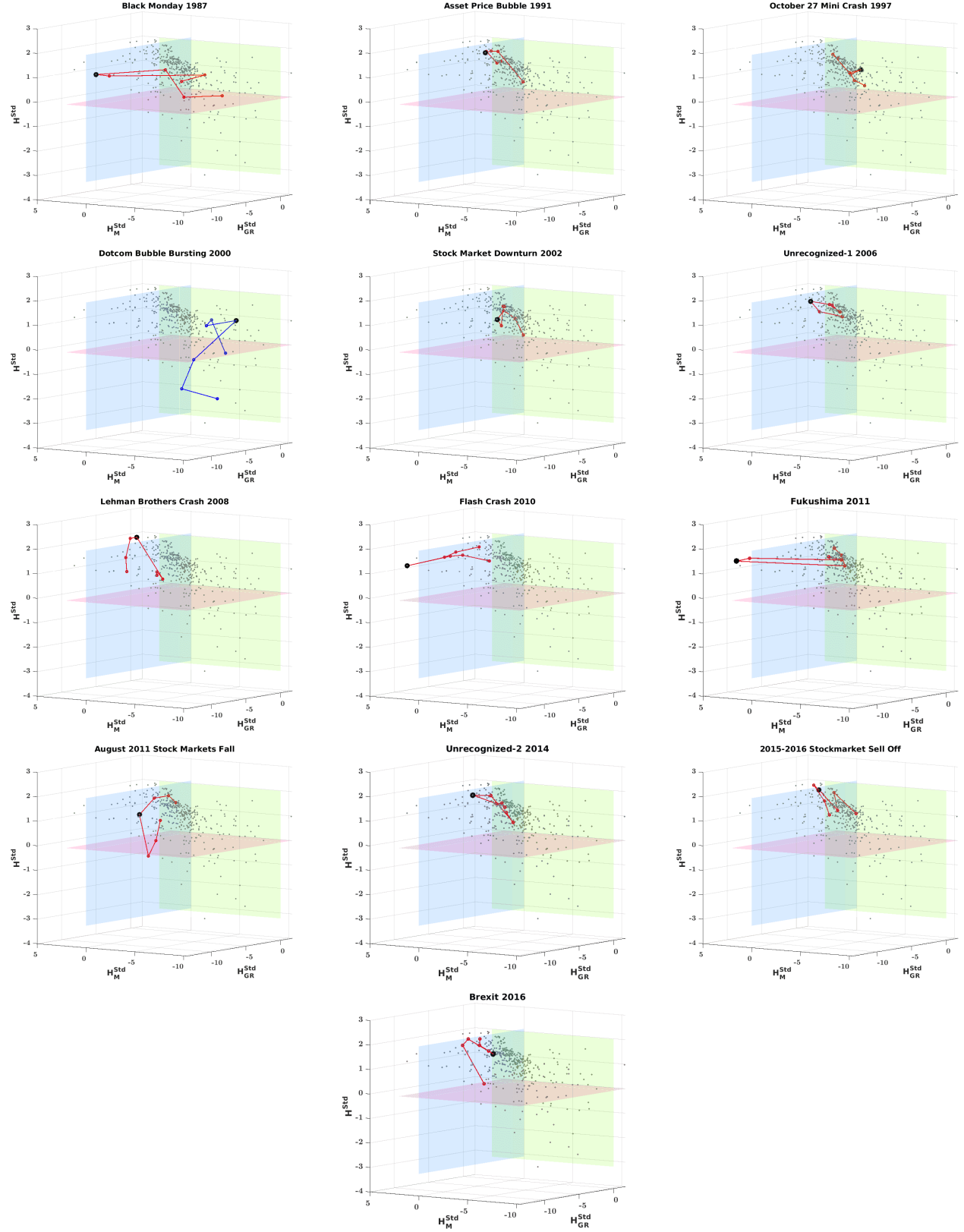


Figure S6. Evolution around the important events in JPN market. Eigen-entropy H calculated from the correlation matrices: (full) C , market mode C_M and group-random mode C_{GR} for all the frames (epoch $M = 40$ days and shift $\Delta = 20$ days) over a period of 1985-2016 of JPN (Nikkei-225). Three co-ordinates axes H^{std} , H_M^{std} and H_{GR}^{std} are the standardized variables, same as Fig. S5. Plots show thirteen important events from the history. Bubbles are connected with blue line and other critical events with red lines. The frame containing the important event is marked with black circle for better visibility.

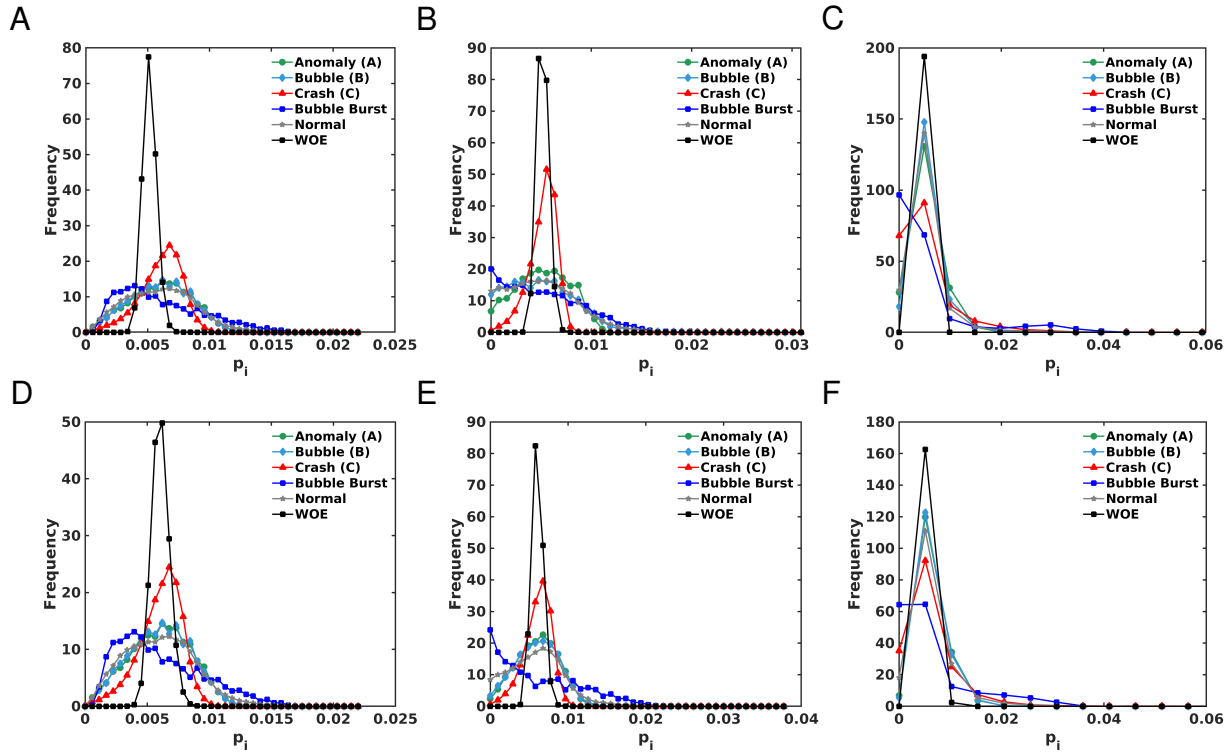


Figure S7. Averaged distributions of the eigen-centralities, showing self-averaging properties. Histograms of the eigen-centralities p_i for anomalies (green circles), bubble (light blue diamonds), bubble bursts (blue squares), crash (red triangles) and normal (grey stars) and WOE (black squares), averaged over the respective ensembles for USA (top row) and for JPN (bottom row). Histograms are evaluated using (A and D) full correlation matrices C and decomposed correlation matrices of (B and E) market mode C_M , and (C and F) group and random mode C_{GR} .

Table S1. List of major crashes and bubbles for USA and JPN markets and their characterization^{42–46}. All the events are plotted in Figs. S5 and S6.

Sl. No	Major crashes and bubbles	Period Date	Region Affected
1	Black Monday	19-10-1987	USA,JPN
2	Friday the 13th Mini Crash	13-10-1989	USA
3	Early 90s Recession	1990	USA
5	Mini Crash Due To Asian Financial Crisis	27-10-1997	USA
6	Lost Decade	2001-2010	JPN
7	9/11 Financial Crisis	11-09-2001	USA,JPN
8	Stock Market Downturn Of 2002	09-10-2002	JPN,USA
9	US Housing Bubble	2005-2007	USA
10	Lehman Brothers Crash	16-09-2008	USA,JPN
11	DJ Flash Crash	06-05-2010	USA,JPN
12	Tsunami/Fukushima	11-03-2011	JPN
13	August 2011 Stock Markets Fall	08-08-2011	USA,JPN
14	Chinese Black Monday and 2015-2016 Sell Off	24-08-2015	USA

Table S2. Values in cross-correlogram of the entropy measures with market parameters

	μ	H	H_M	H_{GR}	$H - H_M$	$-\ln(H - H_M)$	$H - H_{GR}$	VIX	ρ
μ	1	0.361	0.892	-0.392	-0.804	0.987	0.463	0.471	0.619
H	0.361	1	0.313	0.151	0.043	0.387	0.031	0.091	0.164
H_M	0.892	0.313	1	-0.283	-0.935	0.897	0.343	0.336	0.506
H_{GR}	-0.392	0.151	-0.283	1	0.354	-0.314	-0.983	-0.058	-0.41
$H - H_M$	-0.804	0.043	-0.935	0.354	1	-0.799	-0.35	-0.319	-0.471
$-\ln(H - H_M)$	0.987	0.387	0.897	-0.314	-0.799	1	0.389	0.505	0.59
$H - H_{GR}$	0.463	0.031	0.343	-0.983	-0.35	0.389	1	0.076	0.445
VIX	0.471	0.091	0.336	-0.058	-0.319	0.505	0.076	1	0.633
ρ	0.619	0.164	0.506	-0.41	-0.471	0.59	0.445	0.633	1

extreme events in the financial market, e.g., crises, bubbles, etc. The structural entropy depends on the communities of the network and quantifies the “structural diversity”. The structural entropy measure S varies with the change in the number of communities and its heterogeneity. To calculate the entropy one has to first get the communities in the correlation matrix based network using a community detection algorithm^{47,48}, and look at the normalized sizes of the communities. Then one applies the information theory based entropy formula to compute the value of S .

A major drawback of this method is that there is information loss and arbitrariness in the detection of the community structure from correlation matrix. In order to circumvent the information loss during the conversion of correlation matrices to adjacency matrices, an algorithm⁴⁰ was used that utilizes random matrix theory and eigenvalue decomposition method in order to get a “modularity” matrix directly from a correlation matrix without relying on any arbitrary parameter or a threshold. However, this prescription only manages to detect certain features (based on group or sectoral dynamics of the financial market) and hence the problem of information loss is partially resolved.

The detected communities can be represented by a vector $\bar{\sigma}$ of the length equal to the total number of stocks, whose i^{th} component σ_i denotes the community to which node i was assigned to. In general, $\bar{\sigma}$ can possess values ranging from 1 to M , where M is the total number of communities detected by the algorithm. From this, one can then calculate the probability vector (\bar{P}) by normalizing the sizes of different communities as

$$\bar{P} \equiv \left[\frac{c_1}{N}, \frac{c_2}{N}, \dots, \frac{c_M}{N} \right],$$

where c_i is the size of community i .

On this probability vector \bar{P} , one can apply Shannon entropy formula to obtain an entropy measure, called the structural entropy, as:

$$S \equiv - \sum_{i=1}^M P_i \log(P_i).$$

In Fig. S8, we compare the eigen-entropy H measure with the structural entropy S using the community detection algorithm⁴⁰, where they obtain a modularity matrix directly from a correlation matrix, by applying random matrix theory tools and separating

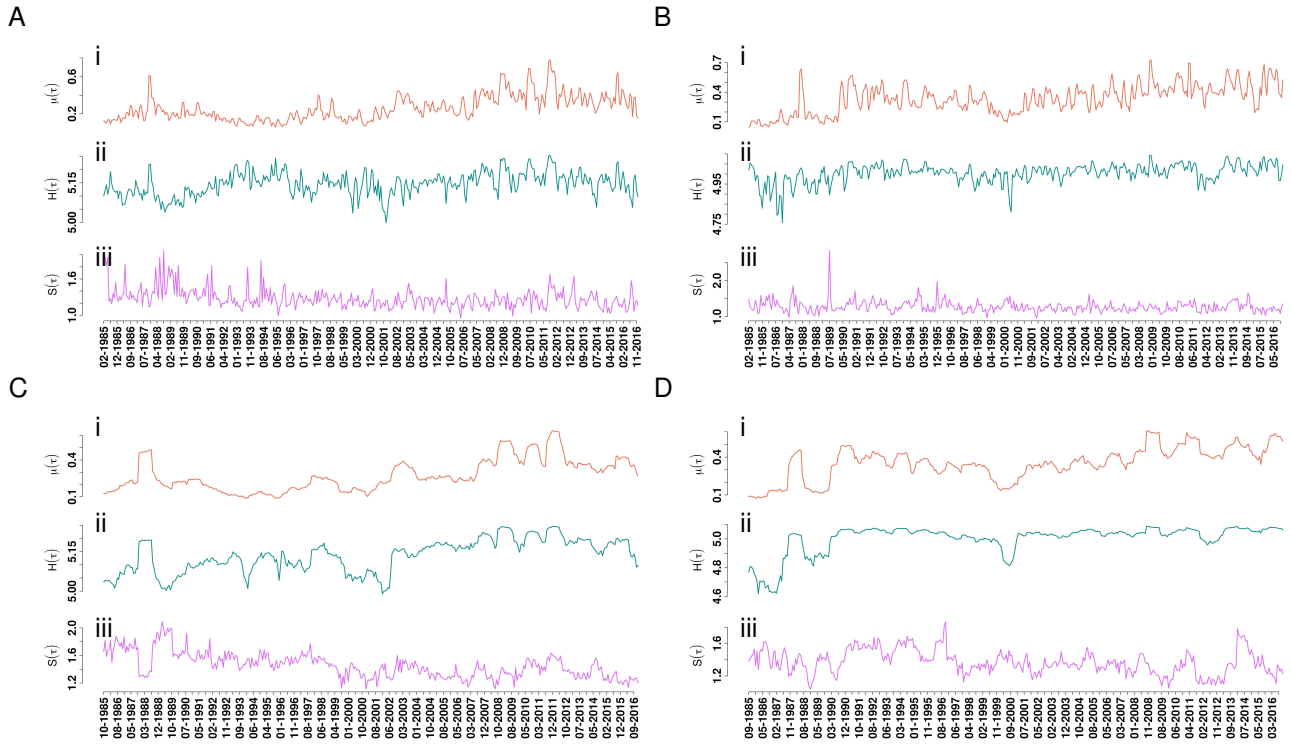


Figure S8. Comparison of eigen-entropy H and structural entropy S . Evolution of (i) average correlation μ , (ii) eigen-entropy H , and (iii) structural entropy S : (A) and (B) $M = 40$ days epoch and $\Delta = 20$ days shift for USA and JPN, respectively, and (C) and (D) $M = 200$ days epoch and $\Delta = 20$ days shift for USA and JPN, respectively.

out just the group mode. The advantage of this method is that a modularity matrix can be supplied directly to a community detection algorithm, without using any arbitrary threshold.

When one compares the two entropy measures, it is evident that the structural entropy is very sensitive to the community detection algorithm (different algorithms yield different community structures). Even the community detection algorithm⁴⁰, which involves identifying the group mode from the correlation matrix is not easy because the boundary (determined by the eigenvalues of the correlation matrix) between the random mode and the group mode, is not distinct (and often arbitrary). In this way, our eigen-entropy measure has an advantage that it is uniquely determined and non-arbitrary (and also has less computational complexity). Also, during a market crash, the structural entropy S behaves differently from the eigen-entropy H , as the market starts behaving like a single (huge) super-community. So, during a crash S (measure of diversity) decreases in contrast to H (measure of disorder or randomness) that increases.

Table S3. List of all stocks of USA market (S&P-500) considered for the analysis. The first column has the serial number, the second column has the abbreviation, the third column has the full name of the stock, and the fourth column specifies the sector as given in the S&P-500.

S.No.	Code	Company Name	Sector	Abbrv
1	CMCSA	Comcast Corp.	Consumer Discretionary	CD
2	DIS	The Walt Disney Company	Consumer Discretionary	CD
3	F	Ford Motor	Consumer Discretionary	CD
4	GPC	Genuine Parts	Consumer Discretionary	CD
5	GPS	Gap Inc.	Consumer Discretionary	CD
6	GT	Goodyear Tire & Rubber	Consumer Discretionary	CD
7	HAS	Hasbro Inc.	Consumer Discretionary	CD
8	HD	Home Depot	Consumer Discretionary	CD
9	HRB	Block H&R	Consumer Discretionary	CD
10	IPG	Interpublic Group	Consumer Discretionary	CD
11	JCP	J. C. Penney Company, Inc.	Consumer Discretionary	CD
12	JWN	Nordstrom	Consumer Discretionary	CD
13	LEG	Leggett & Platt	Consumer Discretionary	CD
14	LEN	Lennar Corp.	Consumer Discretionary	CD
15	LOW	Lowe's Cos.	Consumer Discretionary	CD
16	MAT	Mattel Inc.	Consumer Discretionary	CD
17	MCD	McDonald's Corp.	Consumer Discretionary	CD
18	NKE	Nike	Consumer Discretionary	CD
19	SHW	Sherwin-Williams	Consumer Discretionary	CD
20	TGT	Target Corp.	Consumer Discretionary	CD
21	VFC	V.F. Corp.	Consumer Discretionary	CD
22	WHR	Whirlpool Corp.	Consumer Discretionary	CD
23	ADM	Archer-Daniels-Midland Co	Consumer Staples	CS
24	AVP	Avon Products, Inc.	Consumer Staples	CS
25	CAG	Conagra Brands	Consumer Staples	CS
26	CL	Colgate-Palmolive	Consumer Staples	CS
27	CPB	Campbell Soup	Consumer Staples	CS
28	CVS	CVS Health	Consumer Staples	CS
29	GIS	General Mills	Consumer Staples	CS
30	HRL	Hormel Foods Corp.	Consumer Staples	CS
31	HSY	The Hershey Company	Consumer Staples	CS
32	K	Kellogg Co.	Consumer Staples	CS
33	KMB	Kimberly-Clark	Consumer Staples	CS
34	KO	Coca-Cola Company (The)	Consumer Staples	CS
35	KR	Kroger Co.	Consumer Staples	CS
36	MKC	McCormick & Co.	Consumer Staples	CS
37	MO	Altria Group Inc	Consumer Staples	CS
38	SYT	Sysco Corp.	Consumer Staples	CS
39	TAP	Molson Coors Brewing Company	Consumer Staples	CS
40	TSN	Tyson Foods	Consumer Staples	CS
41	WMT	Wal-Mart Stores	Consumer Staples	CS
42	APA	Apache Corporation	Energy	EG
43	COP	ConocoPhillips	Energy	EG
44	CVX	Chevron Corp.	Energy	EG
45	ESV	Enscopl	Energy	EG
46	HAL	Halliburton Co.	Energy	EG
47	HES	Hess Corporation	Energy	EG
48	HP	Helmerich & Payne	Energy	EG
49	MRO	Marathon Oil Corp.	Energy	EG
50	MUR	Murphy Oil Corporation	Energy	EG

51	NBL	Noble Energy Inc	Energy	EG
52	NBR	Nabors Industries Ltd.	Energy	EG
53	SLB	Schlumberger Ltd.	Energy	EG
54	TSO	Tesoro Corp	Energy	EG
55	VLO	Valero Energy	Energy	EG
56	WMB	Williams Cos.	Energy	EG
57	XOM	Exxon Mobil Corp.	Energy	EG
58	AFL	AFLAC Inc	Financials	FN
59	AIG	American International Group, Inc.	Financials	FN
60	AON	Aon plc	Financials	FN
61	AXP	American Express Co	Financials	FN
62	BAC	Bank of America Corp	Financials	FN
63	BBT	BB&T Corporation	Financials	FN
64	BEN	Franklin Resources	Financials	FN
65	BK	The Bank of New York Mellon Corp.	Financials	FN
66	C	Citigroup Inc.	Financials	FN
67	CB	Chubb Limited	Financials	FN
68	CINF	Cincinnati Financial	Financials	FN
69	CMA	Comerica Inc.	Financials	FN
70	EFX	Equifax Inc.	Financials	FN
71	FHN	First Horizon National Corporation	Financials	FN
72	HBAN	Huntington Bancshares	Financials	FN
73	HCN	Welltower Inc.	Financials	FN
74	HST	Host Hotels & Resorts, Inc.	Financials	FN
75	JPM	JPMorgan Chase & Co.	Financials	FN
76	L	Loews Corp.	Financials	FN
77	LM	Legg Mason, Inc.	Financials	FN
78	LNC	Lincoln National	Financials	FN
79	LUK	Leucadia National Corp.	Financials	FN
80	MMC	Marsh & McLennan	Financials	FN
81	MTB	M&T Bank Corp.	Financials	FN
82	PSA	Public Storage	Financials	FN
83	SLM	SLM Corporation	Financials	FN
84	TMK	Torchmark Corp.	Financials	FN
85	TRV	The Travelers Companies Inc.	Financials	FN
86	USB	U.S. Bancorp	Financials	FN
87	VNO	Vornado Realty Trust	Financials	FN
88	WFC	Wells Fargo	Financials	FN
89	WY	Weyerhaeuser Corp.	Financials	FN
90	ZION	Zions Bancorp	Financials	FN
91	ABT	Abbott Laboratories	Health Care	HC
92	AET	Aetna Inc	Health Care	HC
93	AMGN	Amgen Inc	Health Care	HC
94	BAX	Baxter International Inc.	Health Care	HC
95	BCR	Bard (C.R.) Inc.	Health Care	HC
96	BDX	Becton Dickinson	Health Care	HC
97	BMJ	Bristol-Myers Squibb	Health Care	HC
98	CAH	Cardinal Health Inc.	Health Care	HC
99	CI	CIGNA Corp.	Health Care	HC
100	HUM	Humana Inc.	Health Care	HC

101	JNJ	Johnson & Johnson	Health Care	HC
102	LLY	Lilly (Eli) & Co.	Health Care	HC
103	MDT	Medtronic plc	Health Care	HC
104	MRK	Merck & Co.	Health Care	HC
105	MYL	Mylan N.V.	Health Care	HC
106	SYK	Stryker Corp.	Health Care	HC
107	THC	Tenet Healthcare Corp	Health Care	HC
108	TMO	Thermo Fisher Scientific	Health Care	HC
109	UNH	United Health Group Inc.	Health Care	HC
110	VAR	Varian Medical Systems	Health Care	HC
111	AVY	Avery Dennison Corp	Industrials	ID
112	BA	Boeing Company	Industrials	ID
113	CAT	Caterpillar Inc.	Industrials	ID
114	CMI	Cummins Inc.	Industrials	ID
115	CSX	CSX Corp.	Industrials	ID
116	CTAS	Cintas Corporation	Industrials	ID
117	DE	Deere & Co.	Industrials	ID
118	DHR	Danaher Corp.	Industrials	ID
119	DNB	The Dun & Bradstreet Corporation	Industrials	ID
120	DOV	Dover Corp.	Industrials	ID
121	EMR	Emerson Electric Company	Industrials	ID
122	ETN	Eaton Corporation	Industrials	ID
123	EXPD	Expeditors International	Industrials	ID
124	FDX	FedEx Corporation	Industrials	ID
125	FLS	Flowserve Corporation	Industrials	ID
126	GD	General Dynamics	Industrials	ID
127	GE	General Electric	Industrials	ID
128	GLW	Corning Inc.	Industrials	ID
129	GWV	Grainger (W.W.) Inc.	Industrials	ID
130	HON	Honeywell Int'l Inc.	Industrials	ID
131	IR	Ingersoll-Rand PLC	Industrials	ID
132	ITW	Illinois Tool Works	Industrials	ID
133	JEC	Jacobs Engineering Group	Industrials	ID
134	LMT	Lockheed Martin Corp.	Industrials	ID
135	LUV	Southwest Airlines	Industrials	ID
136	MAS	Masco Corp.	Industrials	ID
137	MMM	3M Company	Industrials	ID
138	ROK	Rockwell Automation Inc.	Industrials	ID
139	RTN	Raytheon Co.	Industrials	ID
140	TXT	Textron Inc.	Industrials	ID
141	UNP	Union Pacific	Industrials	ID
142	UTX	United Technologies	Industrials	ID
143	AAPL	Apple Inc.	Information Technology	IT
144	ADI	Analog Devices, Inc.	Information Technology	IT
145	ADP	Automatic Data Processing	Information Technology	IT
146	AMAT	Applied Materials Inc	Information Technology	IT
147	AMD	Advanced Micro Devices Inc	Information Technology	IT
148	CA	CA, Inc.	Information Technology	IT
149	HPQ	HP Inc.	Information Technology	IT
150	HRS	Harris Corporation	Information Technology	IT

151	IBM	International Business Machines	Information Technology	IT
152	INTC	Intel Corp.	Information Technology	IT
153	KLAC	KLA-Tencor Corp.	Information Technology	IT
154	LRCX	Lam Research	Information Technology	IT
155	MSI	Motorola Solutions Inc.	Information Technology	IT
156	MU	Micron Technology	Information Technology	IT
157	TSS	Total System Services, Inc.	Information Technology	IT
158	TXN	Texas Instruments	Information Technology	IT
159	WDC	Western Digital	Information Technology	IT
160	XXRX	Xerox Corp.	Information Technology	IT
161	AA	Alcoa Corporation	Materials	MT
162	APD	Air Products & Chemicals Inc	Materials	MT
163	BLL	Ball Corp	Materials	MT
164	BMS	Bemis Company, Inc.	Materials	MT
165	CLF	Cleveland-Cliffs Inc.	Materials	MT
166	DD	DuPont	Materials	MT
167	ECL	Ecolab Inc.	Materials	MT
168	FMC	FMC Corporation	Materials	MT
169	IFF	Intl Flavors & Fragrances	Materials	MT
170	IP	International Paper	Materials	MT
171	NEM	Newmont Mining Corporation	Materials	MT
172	PPG	PPG Industries	Materials	MT
173	VMC	Vulcan Materials	Materials	MT
174	CTL	CenturyLink Inc	Telecommunication Services	TC
175	FTR	Frontier Communications Corporation	Telecommunication Services	TC
176	S	Sprint Nextel Corp.	Telecommunication Services	TC
177	T	AT&T Inc	Telecommunication Services	TC
178	VZ	Verizon Communications	Telecommunication Services	TC
179	AEP	American Electric Power	Utilities	UT
180	CMS	CMS Energy	Utilities	UT
181	CNP	CenterPoint Energy	Utilities	UT
182	D	Dominion Energy	Utilities	UT
183	DTE	DTE Energy Co.	Utilities	UT
184	ED	Consolidated Edison	Utilities	UT
185	EIX	Edison Int'l	Utilities	UT
186	EQT	EQT Corporation	Utilities	UT
187	ETR	Entergy Corp.	Utilities	UT
188	EXC	Exelon Corp.	Utilities	UT
189	NEE	NextEra Energy	Utilities	UT
190	NI	NiSource Inc.	Utilities	UT
191	PNW	Pinnacle West Capital	Utilities	UT
192	SO	Southern Co.	Utilities	UT
193	WEC	Wec Energy Group Inc	Utilities	UT
194	XEL	Xcel Energy Inc	Utilities	UT

Table S4. List of all stocks of Japan market (Nikkei-225) considered for the analysis. The first column has the serial number, the second column has the abbreviation, the third column has the full name of the stock, and the fourth column specifies the sector as given in the Nikkei-225.

S.No.	Code	Company Name	Sector	Abbrev
1	S-8801	mitsui fudosan co., ltd.	Capital Goods	CG
2	S-8802	mitsubishi estate co., ltd.	Capital Goods	CG
3	S-8804	tokyo tatemono co., ltd.	Capital Goods	CG
4	S-8830	sumitomo realty & development co., ltd.	Capital Goods	CG
5	S-7003	mitsui eng. & shipbuild. co., ltd.	Capital Goods	CG
6	S-7012	kawasaki heavy ind., ltd.	Capital Goods	CG
7	S-9202	ana holdings inc.	Capital Goods	CG
8	S-1801	taisei corp.	Capital Goods	CG
9	S-1802	obayashi corp.	Capital Goods	CG
10	S-1803	shimizu corp.	Capital Goods	CG
11	S-1808	haseko corp.	Capital Goods	CG
12	S-1812	Kajima Corp.	Capital Goods	CG
13	S-1925	daiwa house ind. co., ltd.	Capital Goods	CG
14	S-1928	sekisui house, ltd.	Capital Goods	CG
15	S-1963	jgc corp.	Capital Goods	CG
16	S-5631	the japan steel works, ltd.	Capital Goods	CG
17	S-6103	okuma corp.	Capital Goods	CG
18	S-6113	amada holdings co., ltd.	Capital Goods	CG
19	S-6301	komatsu ltd.	Capital Goods	CG
20	S-6302	sumitomo heavy ind., ltd.	Capital Goods	CG
21	S-6305	hitachi const. mach. co., ltd.	Capital Goods	CG
22	S-6326	kubota corp.	Capital Goods	CG
23	S-6361	ebara corp.	Capital Goods	CG
24	S-6366	chiyoda corp.	Capital Goods	CG
25	S-6367	daikin industries, ltd.	Capital Goods	CG
26	S-6471	nsk ltd.	Capital Goods	CG
27	S-6472	ntn corp.	Capital Goods	CG
28	S-6473	jtekt corp.	Capital Goods	CG
29	S-7004	hitachi zosen corp.	Capital Goods	CG
30	S-7011	mitsubishi heavy ind., ltd.	Capital Goods	CG
31	S-7013	ihi corp.	Capital Goods	CG
32	S-7911	toppan printing co., ltd.	Capital Goods	CG
33	S-7912	dai nippon printing co., ltd.	Capital Goods	CG
34	S-7951	yamaha corp.	Capital Goods	CG
35	S-1332	nippon suisan kaisha, ltd.	Consumer Goods	CN
36	S-2002	nisshin seifun group inc.	Consumer Goods	CN
37	S-2282	nh foods ltd.	Consumer Goods	CN
38	S-2501	sapporo holdings ltd.	Consumer Goods	CN
39	S-2502	asaahi group holdings, ltd.	Consumer Goods	CN
40	S-2503	kirin holdings co., ltd.	Consumer Goods	CN
41	S-2531	takara holdings inc.	Consumer Goods	CN
42	S-2801	kikkoman corp.	Consumer Goods	CN
43	S-2802	ajinomoto co., inc.	Consumer Goods	CN
44	S-2871	nichirei corp.	Consumer Goods	CN
45	S-8233	takashimaya co., ltd.	Consumer Goods	CN
46	S-8252	marui group co., ltd.	Consumer Goods	CN
47	S-8267	aeon co., ltd.	Consumer Goods	CN
48	S-9602	toho co., ltd	Consumer Goods	CN
49	S-9681	tokyo dome corp.	Consumer Goods	CN
50	S-9735	secom co., ltd.	Consumer Goods	CN

51	S-8331	THE CHIBA BANK, LTD.	Financials	FN
52	S-8355	THE SHIZUOKA BANK, LTD.	Financials	FN
53	S-8253	CREDIT SAISON CO., LTD.	Financials	FN
54	S-8601	DAIWA SECURITIES GROUP INC.	Financials	FN
55	S-8604	NOMURA HOLDINGS, INC.	Financials	FN
56	S-3405	KURARAY CO., LTD.	Materials	MT
57	S-3407	ASAHI KASEI CORP.	Materials	MT
58	S-4004	SHOWA DENKO K.K.	Materials	MT
59	S-4005	SUMITOMO CHEMICAL CO., LTD.	Materials	MT
60	S-4021	NISSAN CHEMICAL IND., LTD.	Materials	MT
61	S-4042	TOSOH CORP.	Materials	MT
62	S-4043	TOKUYAMA CORP.	Materials	MT
63	S-4061	DENKA CO., LTD.	Materials	MT
64	S-4063	SHIN-ETSU CHEMICAL CO., LTD.	Materials	MT
65	S-4183	MITSUI CHEMICALS, INC.	Materials	MT
66	S-4208	UBE INDUSTRIES, LTD.	Materials	MT
67	S-4272	NIPPON KAYAKU CO., LTD.	Materials	MT
68	S-4452	KAO CORP.	Materials	MT
69	S-4901	FUJIFILM HOLDINGS CORP.	Materials	MT
70	S-4911	SHISEIDO CO., LTD.	Materials	MT
71	S-6988	NITTO DENKO CORP.	Materials	MT
72	S-5002	SHOWA SHELL SEKIYU K.K.	Materials	MT
73	S-5201	ASAHI GLASS CO., LTD.	Materials	MT
74	S-5202	NIPPON SHEET GLASS CO., LTD.	Materials	MT
75	S-5214	NIPPON ELECTRIC GLASS CO., LTD.	Materials	MT
76	S-5232	SUMITOMO OSAKA CEMENT CO., LTD.	Materials	MT
77	S-5233	TAIHEIYO CEMENT CORP.	Materials	MT
78	S-5301	TOKAI CARBON CO., LTD.	Materials	MT
79	S-5332	TOTO LTD.	Materials	MT
80	S-5333	NGK INSULATORS, LTD.	Materials	MT
81	S-5706	MITSUI MINING & SMELTING CO.	Materials	MT
82	S-5707	TOHO ZINC CO., LTD.	Materials	MT
83	S-5711	MITSUBISHI MATERIALS CORP.	Materials	MT
84	S-5713	SUMITOMO METAL MINING CO., LTD.	Materials	MT
85	S-5714	DOWA HOLDINGS CO., LTD.	Materials	MT
86	S-5715	FURUKAWA CO., LTD.	Materials	MT
87	S-5801	FURUKAWA ELECTRIC CO., LTD.	Materials	MT
88	S-5802	SUMITOMO ELECTRIC IND., LTD.	Materials	MT
89	S-5803	FUJIKURA LTD.	Materials	MT
90	S-5901	TOYO SEIKAN GROUP HOLDINGS, LTD.	Materials	MT
91	S-3865	HOKUETSU KISHU PAPER CO., LTD.	Materials	MT
92	S-3861	OJI HOLDINGS CORP.	Materials	MT
93	S-5101	THE YOKOHAMA RUBBER CO., LTD.	Materials	MT
94	S-5108	BRIDGESTONE CORP.	Materials	MT
95	S-5401	NIPPON STEEL & SUMITOMO METAL CORP.	Materials	MT
96	S-5406	KOBE STEEL, LTD.	Materials	MT
97	S-5541	PACIFIC METALS CO., LTD.	Materials	MT
98	S-3101	TOYOBO CO., LTD.	Materials	MT
99	S-3103	UNITIKA, LTD.	Materials	MT
100	S-3401	TEIJIN LTD.	Materials	MT

101	S-3402	TORAY INDUSTRIES, INC.	Materials	MT
102	S-8001	ITOCHU CORP.	Materials	MT
103	S-8002	MARUBENI CORP.	Materials	MT
104	S-8015	TOYOTA TSUSHO CORP.	Materials	MT
105	S-8031	mitsui & co., ltd.	Materials	MT
106	S-8053	SUMITOMO CORP.	Materials	MT
107	S-8058	mitsubishi corp.	Materials	MT
108	S-4151	KYOWA HAKKO KIRIN CO., LTD.	Pharmaceuticals	PH
109	S-4503	ASTELLAS PHARMA INC.	Pharmaceuticals	PH
110	S-4506	SUMITOMO DAINIPPON PHARMA CO., LTD.	Pharmaceuticals	PH
111	S-4507	SHIONOGI & CO., LTD.	Pharmaceuticals	PH
112	S-4519	CHUGAI PHARMACEUTICAL CO., LTD.	Pharmaceuticals	PH
113	S-4523	EISAI CO., LTD.	Pharmaceuticals	PH
114	S-7201	NISSAN MOTOR CO., LTD.	Information Technology	IT
115	S-7202	ISUZU MOTORS LTD.	Information Technology	IT
116	S-7205	HINO MOTORS, LTD.	Information Technology	IT
117	S-7261	MAZDA MOTOR CORP.	Information Technology	IT
118	S-7267	HONDA MOTOR CO., LTD.	Information Technology	IT
119	S-7270	SUBARU CORP.	Information Technology	IT
120	S-7272	YAMAHA MOTOR CO., LTD.	Information Technology	IT
121	S-3105	NISSHINBO HOLDINGS INC.	Information Technology	IT
122	S-6479	MINEBEA MITSUMI INC.	Information Technology	IT
123	S-6501	HITACHI, LTD.	Information Technology	IT
124	S-6502	TOSHIBA CORP.	Information Technology	IT
125	S-6503	mitsubishi electric corp.	Information Technology	IT
126	S-6504	FUJI ELECTRIC CO., LTD.	Information Technology	IT
127	S-6506	YASKAWA ELECTRIC CORP.	Information Technology	IT
128	S-6508	MEIDENSHA CORP.	Information Technology	IT
129	S-6701	NEC CORP.	Information Technology	IT
130	S-6702	FUJITSU LTD.	Information Technology	IT
131	S-6703	OKI ELECTRIC IND. CO., LTD.	Information Technology	IT
132	S-6752	PANASONIC CORP.	Information Technology	IT
133	S-6758	SONY CORP.	Information Technology	IT
134	S-6762	TDK CORP.	Information Technology	IT
135	S-6770	ALPS ELECTRIC CO., LTD.	Information Technology	IT
136	S-6773	PIONEER CORP.	Information Technology	IT
137	S-6841	YOKOGAWA ELECTRIC CORP.	Information Technology	IT
138	S-6902	DENSO CORP.	Information Technology	IT
139	S-6952	CASIO COMPUTER CO., LTD.	Information Technology	IT
140	S-6954	FANUC CORP.	Information Technology	IT
141	S-6971	KYOCERA CORP.	Information Technology	IT
142	S-6976	TAIYO YUDEN CO., LTD.	Information Technology	IT
143	S-7752	RICOH CO., LTD.	Information Technology	IT
144	S-8035	TOKYO ELECTRON LTD.	Information Technology	IT
145	S-4543	TERUMO CORP.	Information Technology	IT
146	S-4902	KONICA MINOLTA, INC.	Information Technology	IT
147	S-7731	NIKON CORP.	Information Technology	IT
148	S-7733	OLYMPUS CORP.	Information Technology	IT
149	S-7762	CITIZEN WATCH CO., LTD.	Information Technology	IT
150	S-9501	TOKYO ELECTRIC POWER COMPANY HOLDINGS, I	Transportation & Utilities	TU

151	S-9502	CHUBU ELECTRIC POWER CO., INC.	Transportation & Utilities	TU
152	S-9503	THE KANSAI ELECTRIC POWER CO., INC.	Transportation & Utilities	TU
153	S-9531	TOKYO GAS CO., LTD.	Transportation & Utilities	TU
154	S-9532	OSAKA GAS CO., LTD.	Transportation & Utilities	TU
155	S-9062	NIPPON EXPRESS CO., LTD.	Transportation & Utilities	TU
156	S-9064	YAMATO HOLDINGS CO., LTD.	Transportation & Utilities	TU
157	S-9101	NIPPON YUSEN K.K.	Transportation & Utilities	TU
158	S-9104	MITSUMI O.S.K.LINES, LTD.	Transportation & Utilities	TU
159	S-9107	KAWASAKI KISEN KAISHA, LTD.	Transportation & Utilities	TU
160	S-9001	TOBU RAILWAY CO., LTD.	Transportation & Utilities	TU
161	S-9005	TOKYU CORP.	Transportation & Utilities	TU
162	S-9007	ODAKYU ELECTRIC RAILWAY CO., LTD.	Transportation & Utilities	TU
163	S-9008	KEIO CORP.	Transportation & Utilities	TU
164	S-9009	KEISEI ELECTRIC RAILWAY CO., LTD.	Transportation & Utilities	TU
165	S-9301	MITSUBISHI LOGISTICS CORP.	Transportation & Utilities	TU